A Dissertation

by

Alev CETIN

Graduate School of Health Science, Anadolu University

Master of Science

GENERAL ASPECT TO DRUGS FOR USED NIEMANN-PICK DISEASE, THEIR MECHANISM OF ACTION AND DESIGN OF NEW POTENTIAL DRUGS

GENERAL ASPECT TO DRUGS FOR USED NIEMANN-PICK DISEASE, THEIR MECHANISM OF ACTION AND DESIGN OF NEW POTENTIAL DRUGS

A Dissertation

by

Alev CETIN

Graduate School of Health Science, Anadolu University

Master of Science

Thesis Advisors:

Assoc. Prof. Dr. Asiye MERIC

Assoc. Prof. Dr. Antonio CARRIERI

September 2013

Eskisehir

This studying entitled **"GENERAL ASPECT TO DRUGS FOR USED NIEMANN-PICK DISEASE, THEIR EFFECT MECHANISMS AND DESIGN OF NEW POTENTIAL DRUGS"**, which is prepared by Alev CETIN as a Master degree's dissertation, is approved evaluating in accordance with the relevant provisions of Regulation Postgraduate Education.

11/09/2013

Approved by:

Assoc. Prof. Dr. Asiye MERIC

Assoc. Prof. Dr. Antonio CARRIERI

Prof. Dr. Rahime SIMSEK

Assoc. Prof. Dr. Yusuf OZKAY

This dissertation is approved by Board of Director of Anadolu University Graduate School of Health Science on 11th of September, 2013 with decision number .....

Director of Graduate School of Health Science

NIEMANN-PICK HASTALIĞINDA KULLANILAN İLAÇLARA GENEL BAKIŞ, ETKİ MEKANİZMALARI VE YENİ POTANSİYEL İLAÇLARIN TASARLANMASI

ÖZET

Niemann-Pick hastalığı, genetik mutasyonlara sebep olan ve metabolizmayı olumsuz yönde etkileyen lizozomal depo hastalıklarından birisidir. Tip A, B, C ve D olmak üzere dört çeşittir. Niemann-Pick Tip C ve D, metabolik temelde genetik olarak Niemann-Pick Tip A ve B' den farklıdır.

Canlı hücrelerde LDL-indüklü kolesteril esterlerin oluşumunun engellenmesi ya da gecikmesi nedeniyle endosite LDL-türevi kolesterolün lizozomal/geç endozomal organellerdeki birikimi, Niemann-Pick Tip C lezyonunun fenotipik bir damgası olduğu düşünülmektedir.

Lizozomal depo organlarında kolesterol miktarındaki azalma şu mekanizmalardan birisi veya kombinasyonları ile mümkün olabilir: (1) lizozomlardan kolesterol çıkışını arttırmak; (2) kolesterol alımını azaltmak; (3) kolesteril esterlerinin LAL tarafından hidrolizini azaltmak.

2. Mekanizmanın gerçekleşmesi için şu iki seçenek uygun olabilir: (1) NPC1L1 inhibisyonu ile absorblanan kolesterol seviyesinin azaltılması; (2) NPC1L1 gen ekspresyonunun aşağı-regülasyonu (down-regulation).

Önceki çalışmalar *in vitro* ortamda insan ve hayvan modellerinde NPC1L1 gen ekspresyonu aşağı-regülasyonunun, PPAR'ların aktivasyonu ile mümkün olduğunu göstermiştir. Bu çalışmada 2. seçenek değerlendirilmiş ve NPC hastalığı için olası bir tedavi keşfetmek amacıyla PPAR agonistleri üzerinde çalışılmıştır. Yeni bir yapı iskeleti oluşturmak maksadıyla, PPAR agonistleri olarak fibratların en çok bilinen ve çalışılan gruplardan biri olması nedeniyle klofibrattan türetilen AL26-18'in modifikasyonu ile **Molekül 1**, **1a**, **2**, **2a**, **3**, **4**, **5**, **5a** ve **6** sentezlenmiştir. Bu lider bileşik üzerinde özellikle aromatik kısmın

modifikasyonuna ve izoster moleküllerin (**Comp. 1a**, **2a** ve **5a**) sentezine odaklanılmıştır.

Biyolojik aktivite sonuçları AL26-18 (**Comp. 1**)' e göre kıyaslandıklarında, hedef moleküllerin yarışmalı bir şekilde tam olarak PPARαve kısmi olarak PPARγ üzerinde etkili olduklarını göstermiştir. Hatta bazı moleküllerin PPARα üzerindeki aktivasyonunun referans molekülden daha iyi olduğu kanıtlanmıştır. Bu çalışmalara göre, hedef moleküllerin bazıları NPC hastalığının tedavisinde etkili olabilir.

Anahtar Kelimeler: Niemann–Pick tip C1 (NPC1), PPARs, klofibrat

GENERAL ASPECT TO DRUGS FOR USED NIEMANN-PICK DISEASE, THEIR MECHANISM OF ACTION AND DESIGN OF NEW POTENTIAL DRUGS

ABSTRACT

Niemann-Pick disease is one of the lysosomal storage disorders which negatively affect the metabolism and give rise to genetic mutations. There are four forms of this disease: Niemann-Pick Type A, B, C, and D. In contrast, the metabolic basis of Types C and D Niemann–Pick disease, genetically distinct from Niemann–Pick Type A and B.

Lysosomal/late endosomal sequestration of endocytosed low density lipoprotein (LDL)-derived cholesterol is considered the hallmark phenotypic feature of the Niemann-Pick Type C lesion, together with a block or delay of LDL-induced cholesteryl ester formation in living cells.

A decrease in cholesterol content within the LSOs can be possible by one or a combination of the following mechanisms: (1) increase in the cholesterol efflux from the LSOs; (2) decrease in the uptake of cholesterol; (3) decrease in the hydrolysis of cholesteryl esters by LAL.

Considering on the second mechanism to execute might have reasonable two options: (1) decreasing absorbed cholesterol level by inhibition of NPC1L1; (2) down-regulating NPC1L1 gene expression.

Previous studies have shown that down-regulation of NPC1L1 gene expression is possible activations of PPARs *in vitro* both in human and mouse models. In the present study, this second option is evaluated and studied on PPARs agonists for exploring a possible treatment NPC disease. To create a new scaffold **Compound 1**, **1a**, **2**, **2a**, **3**, **4**, **5**, **5a** and **6** were synthesized by modification of AL26-18, lead compound, which had derived from clofibrate due to fibrates are one of the most known-studied group as PPAR agonists. On the lead compound especially has

been focused on the aromatic portion and synthesis of isoster compounds that are **Comp. 1a**, **2a** and **5a** for modification.

Biological activity results show that all compounds have good business competitiveness full or partial, respectively on PPARα and PPARγ, compared to the AL26-18 (**Comp. 1**). In some cases, the activity on PPARα proves to be even better compared to the compounds used as reference. According to these studies, some of these compounds could be effective for treating NPC disease.

Key Words: Niemann–Pick type C1 (NPC1), PPARs, clofibrate

CURRICULUM VITAE

I was born in 1987, Balikesir. After I finished primary, secondary and high school education in Denizli, I graduated from Department of Chemisty, Faculty of Science, Anadolu University (Eskisehir/Turkey) in 2010 as a chemist. Then, I have completed master degree in the same university at Department of Pharmaceutical Chemistry, Health of Science Institution with this dissertation in 2013.

ACKNOWLEDGEMENTS

First, I would like to thank *Dr. Asiye MERIC* for being my mentor. She has encouraged and supported me with her advice and patience in every step in this study.

I would also like to thank *Dr. Antonio CARRIERI* for being my second mentor. He gave me different insight and motivating me with his guidance and willingness. The successful completion of my graduate studies would not have been possible without them.

I am especially grateful to *Dr. Fulvio LOIODICE* and *Dr. Giuseppe FRACCHIOLLA*. They opened the doors of their laboratory to me. This has allowed me great opportunity to expand on my search experience and guidance at Bari University. Without them, my project would have been even more difficult to comprehend.

I thank *Dr. Antonio LAGHEZZA* and *Dr. Paolo TORTORELLA* for their time and candour.

Many thanks go to our collaborators; *Dr. Luca PIEMONTESE* and *Ph.D Sabina SBLANO* who have kindly allowed me to pursue and participate in various projects and have shared their priceless experience.

Finally, I would like to give special thanks to my family, *Esat, Necla* and *Alper CETIN*, for the never ending supports. Especially, I thank to my mom for blindly supporting me while I give all of my life decisions.

TABLE OF CONTENTS

Page

LIST OF FIGURES

Page

LIST OF TABLES

Page

LIST OF ABBREVIATIONS

ACAT	Acyl Co-A/cholesteryl acyl transferase
CAI	Cholesterol-absorption inhibitor
CEs	Cholesterol esters
DBD	DNA binding domain
DMF	Dimethylformamide
ER	Endoplasmic reticulum
Et_2O	Diethyl ether
HDL	High density lipoprotein
HMGCR	3-Hydroxy-3-methylglutaryl-CoA reductase
LAL	Lysosomal acid lipase
LBD	Ligand binding domain
LDL	Low density lipoprotein
LE/LY	Late endosomes/lysosomes
LSO	Lysosomal storage organelle
NaH	Sodium hydride
NaOH	Sodium hydroxide
NPC	Niemann-Pick Type C
NPC1L1	Niemann-Pick C1 Like 1
PPAR	Peroxisome proliferator activated receptor
PPRE	Peroxisome proliferator-response element

PUFA	Polyunsaturated fatty acid
RT	Room Temperature
RXR	Retinoid X receptor
SAR	Structure-activity relationship
SCAP	Sterol regulatory element-binding protein cleavage-activating protein
SSD	Sterol-sensing domain
TES	Triethylsilane
THF	Tetrahydrofuran
TICE	Transintestinal cholesterol efflux
TZD	Thiazolidinedione

INTRODUCTION AND REVIEW OF LITERATURE

1. Lysosomal Storage Diseases

Lipid storage diseases are very lethal group of diseases, common in populations who share same genetic background and are the result of the genetic mutations of enzymes which take part in lipid metabolism. Lipid storage diseases can pass through next generations via genes, usually juvenile-onset and have very progressive ending with the death of the patients before they can reach adult ages (Fig. 1) (Table 1) (Gazioğlu, 2012).

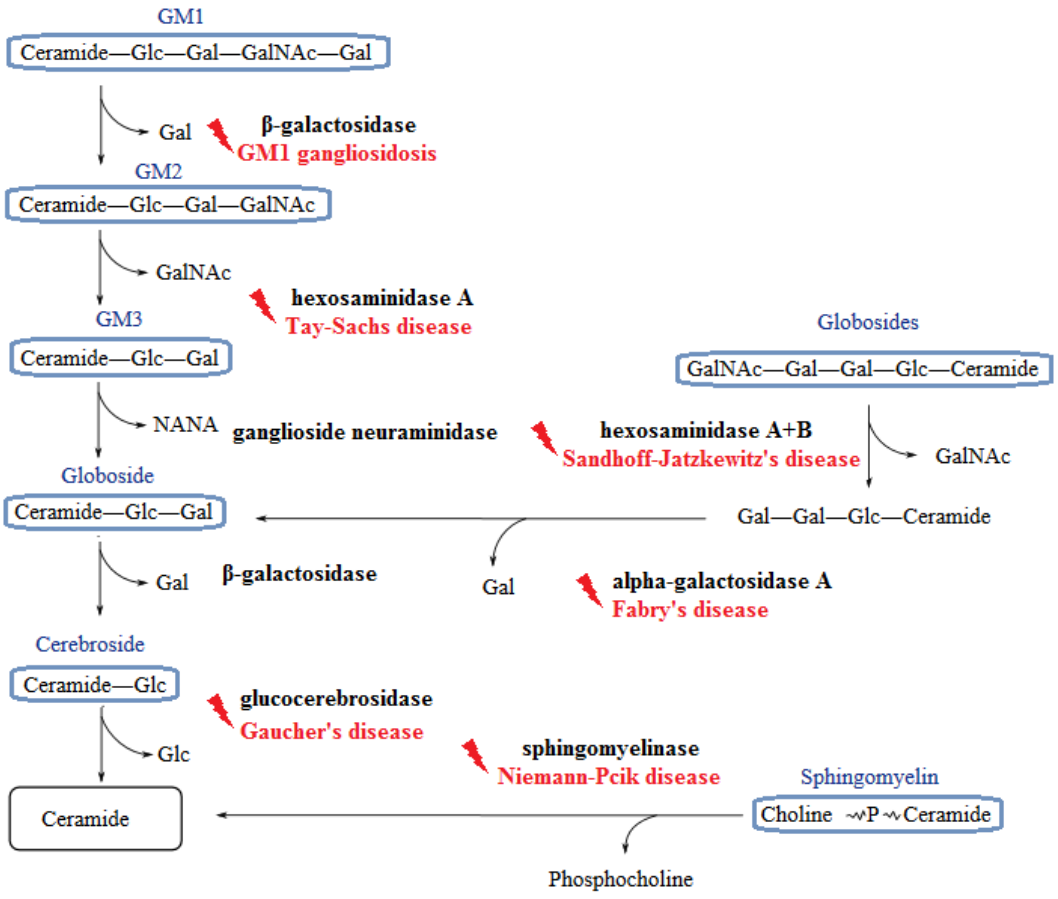

Figure 1. Diseases of as a result of certain enzyme deficiencies (Altınışık, 2006).

Disorder	Enzyme Deficiency	Accumulating Substance	Symptoms
GM_1Gangliosidosis	GM_1ganglioside: β-galaktosidase	GM_1 ganglioside	Mental retardation, skeletal abnormalities, hepatomegaly
Tay-Sachs Disease	Hexosaminidase A	GM_2 ganglioside	Mental retardation, blindness, early mortality
Sandhoff-Jatzkewitz's Disease	Hexosaminidase A and B	Globoside, GM_2 ganglioside	Same symptoms as Tay-Sachs, progresses more rapidly
Fabry's Disease	α-Galactosidase A	Globotriaosylceramide; also called ceramidetrihexoside (CTH)	Kidney failure, skin rashes
Niemann-Pick Disease	Sphingomyelinase	Sphingomyeline	All type lead to mental retardation, hepatosplenomegaly, early fatality potential
Gaucher's Disease	Glucocerebrosidase	Glucocerebrosidase	Hepatosplenomegaly, mental retardation in infantile form, long bone degeneration

Table 1. Enzyme deficiencies, accumulating substances and symptoms of some lysosomal storage diseases (Altınışık, 2006).

Lysosomal storage diseases result from accumulation in lysosomes of metabolites that would normally be degraded by one of the many hydrolytic enzymes which reside in subcellular organelles. These specific enzymes deficiencies of lysosomal storage disease have been identified by product stored in tissues. The natures of these storage products are identified to be sphingolipids and glycosaminoglycans (Gelmez-Beker and Ali Yazıcıoğlu, 2002).

2. Niemann-Pick Disease

Niemann-Pick disease, identified by Albert Niemann in 1914 and published its' pathology in the 1930s by Ludwig Pick, is one of the lysosomal storage disorder which negatively affect the metabolism and give rise to genetic mutations. There are four forms of this disease: Niemann-Pick Type A, B, C, and D; but most of defined in the form of three Types A, B, and C (Gazioğlu, 2012).

Patients with Type A manifest severe neurovisceral disease while patients with Type B have a chronic course with only visceral involvement. In both, massive amounts of sphingomyelin (Fig.2) accumulate in liver and spleen, and a generalized deficiency of sphingomyelinase is characteristic, and the basis for diagnosis (Vanier, 2002). Sphingomyelins are the most common sphingolipids. They are classified as ceramides (Fig.3) with phosphocholine or phosphoethanolamine moiety (Voet and Voet, 2004).

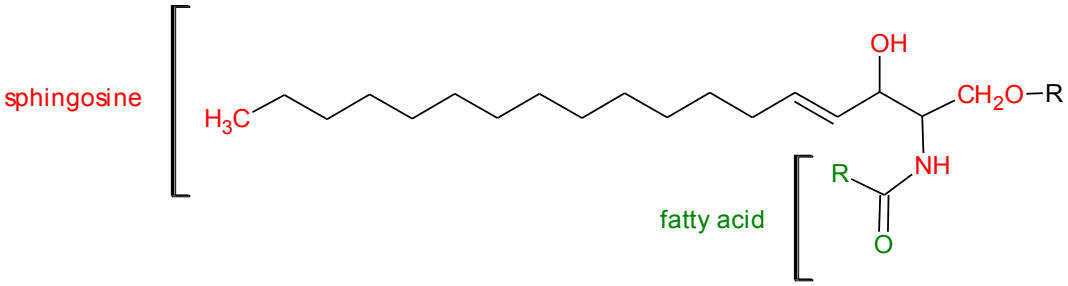

Figure 2. Chemical structure of ceramide molecule (Gazioğlu, 2012).

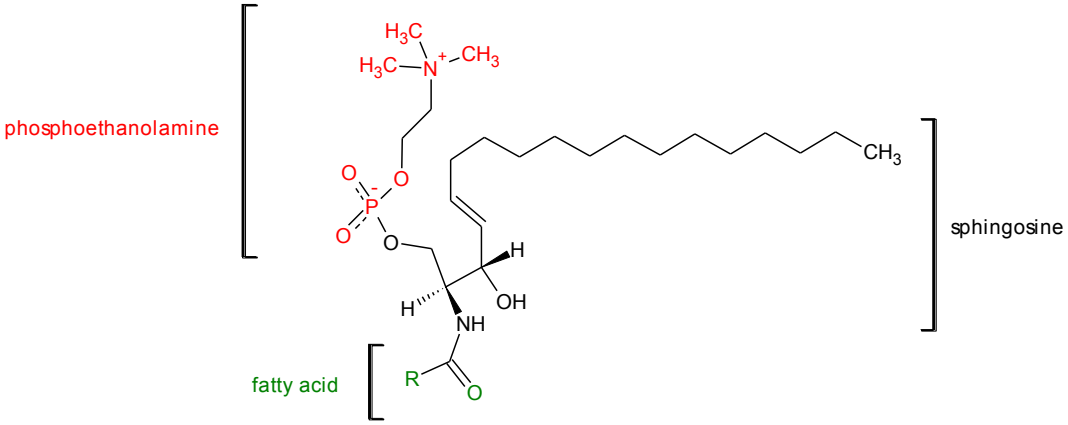

Figure 3. Chemical structure of sphingomyelin (Gazioğlu, 2012).

In contrast, the metabolic basis of Types C and D Niemann–Pick disease, genetically distinct from Niemann–Pick Type A and B, remained an enigma for a long time. The demonstration in the early eighties of abnormalities of intracellular processing of endocytosed cholesterol specific for types C and D facilitated the elucidation of the metabolic and molecular defects and elaboration of a reliable diagnostic strategy. Lysosomal/late endosomal sequestration of endocytosed low density lipoprotein (LDL)-derived cholesterol is considered the hallmark phenotypic feature of the Niemann-Pick Type C lesion, together with a block or delay of LDL-induced cholesteryl ester formation in living cells (Vanier, 2002).

2.1. Niemann-Pick Type C (NPC) Disease

Niemann-Pick Type C disease is a rare, incurable, autosomal recessive lysosomal storage disorder. The disease is characterized by significant accumulation of unesterified cholesterol, glycosphingolipids, and other lipids (Fig.4) within late endosomes/lysosomes (LE/LY). Clinical manifestations include liver abnormalities, epilepsy, seizures, and significant neurodegeneration, ultimately resulting in fatal outcomes (Rosenbaum, *et al.*, 2010).

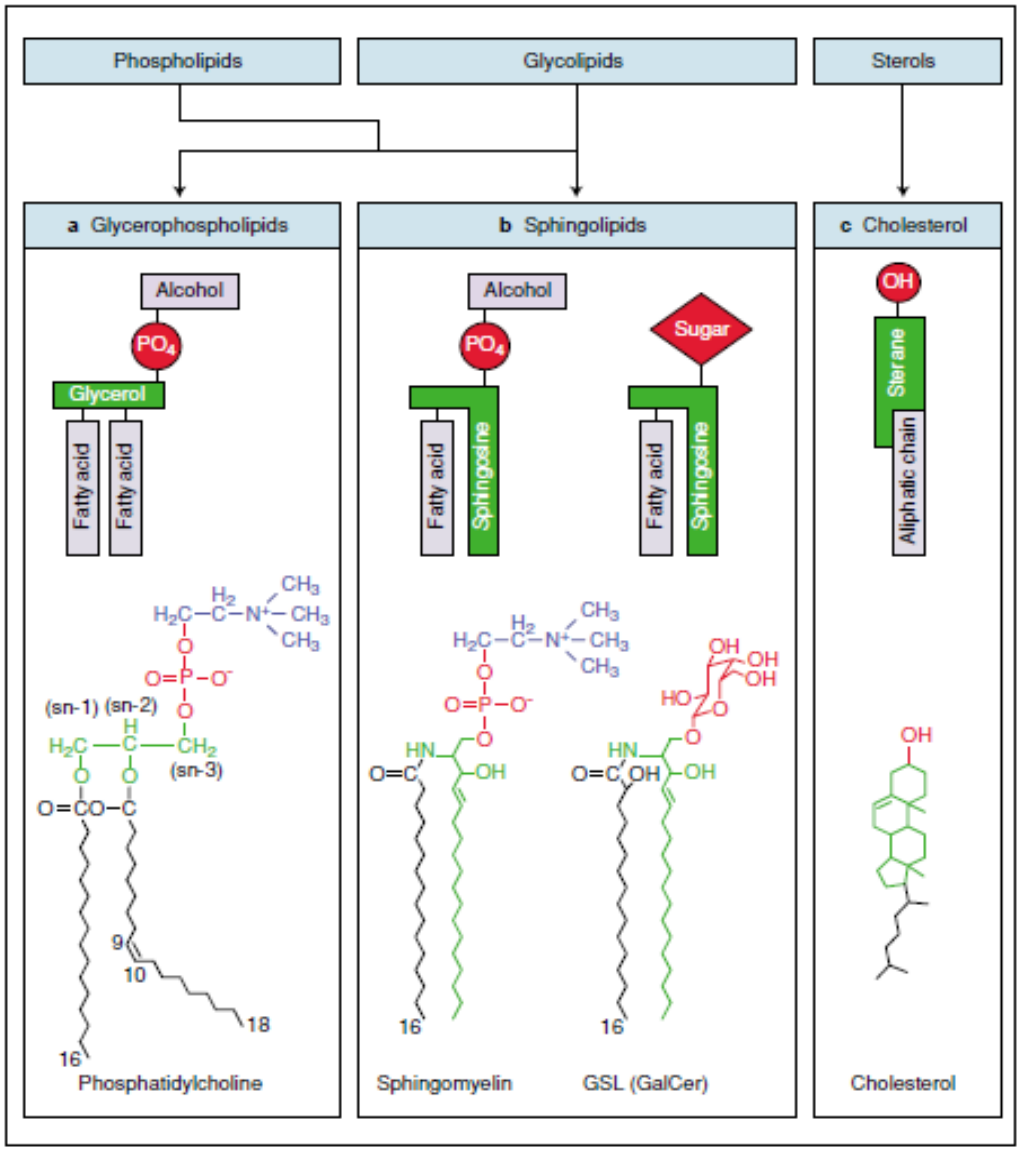

Figure4. Structures of accumulated of unesterified cholesterol, glycosphingolipids, and other lipids in NPC disease (Fantini, *et al.*, 2002)

In normal cells, LDL-associated cholesterol esters (CEs) are transported via receptor-mediated endocytosis to the LE/LY. Within this compartment, lysosomal acid lipase (LAL) hydrolyses CEs to free cholesterol and fatty acids. Free cholesterol is then transported from the LE/LY to various organelles, including the endoplasmic reticulum (ER) and the plasma membrane (Fig.5). LDL receptor-mediated cholesterol uptake, transport to the LE/LY, and cholesteryl ester hydrolysis by LAL are unaltered in NPC-deficient cells. However, the egress of

liberated cholesterol from the LE/LY is significantly reduced, causing them to become lysosomal storage organelles (LSOs). Consequently, re-esterification by acyl Co-A/cholesteryl acyl transferase (ACAT) is reduced (Rosenbaum, *et al.*, 2010).

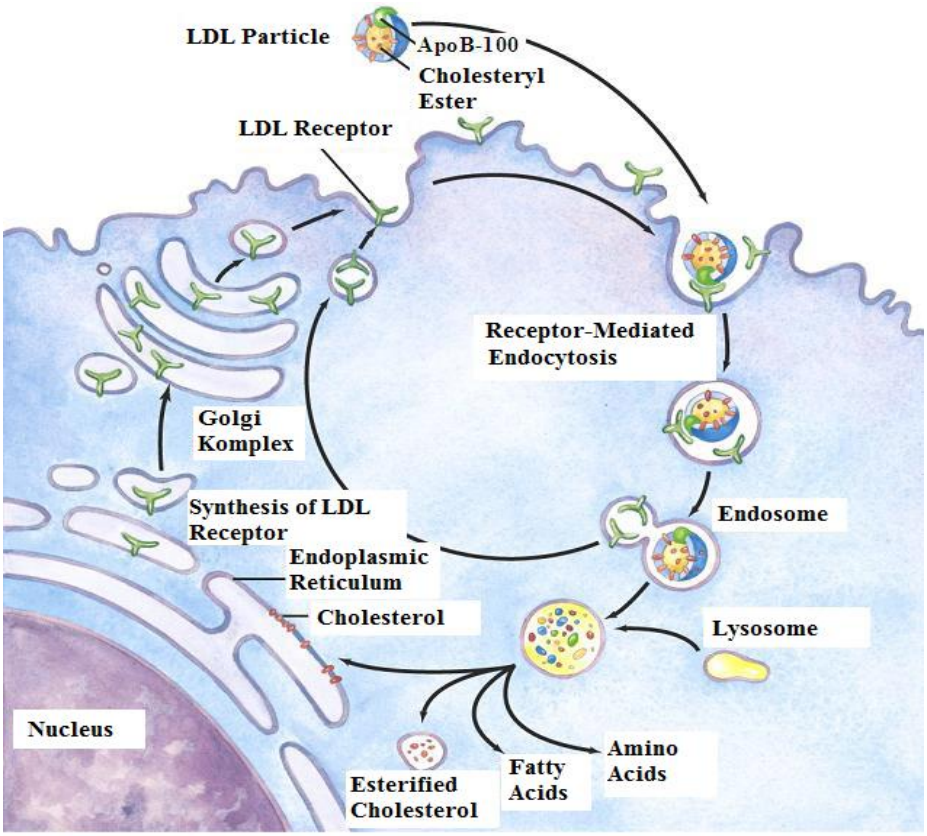

Figure 5. Endocytosis of LDL (Nelson and Cox, 2005).

NPC disease is caused by mutations in one of two genes, *Npc1* (95 % of all cases) and *Npc2*. The *Npc1* gene encodes the 1278-residue integral membrane NPC1 protein, which contains 13 putative transmembrane domains. The *Npc2*gene encodes the soluble protein NPC2. Both proteins are involved in cholesterol trafficking from lysosomes. The current model for NPC1- and NPC2-mediated cholesterol efflux is as follows: after lysosomal hydrolysis of LDL cholesteryl esters, cholesterol binds NPC2, which transfers it to NPC1; subsequently, NPC1 mediates the exit of cholesterol from lysosomes (Vazquez, *et al.*, 2012) (Fig.6).

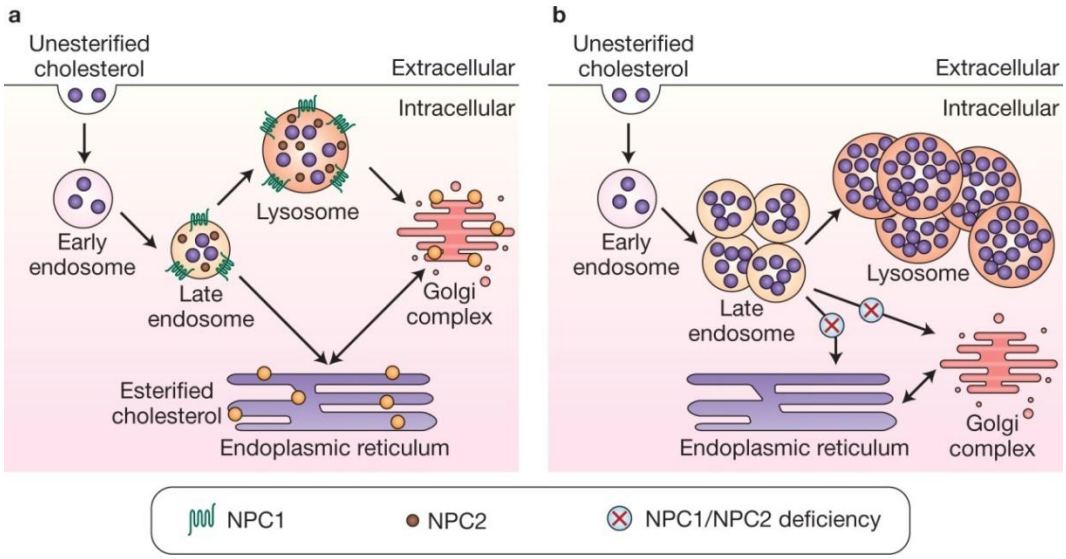

Figure 6. Lipid trafficking defects in Niemann–Pick type C disease. (Pacheco, 2008).

Cosner *et al.* (2009) reported that pyrrolinone family (Fig.7) has dual observation of cholesterol reduction and mild toxicity that made them an attractive target for further investigation as potential therapeutic leads for NPC disease. *N*-Aryl-3-alkylidenepyrrolinones were investigated as potential NPC Disease therapeutics.

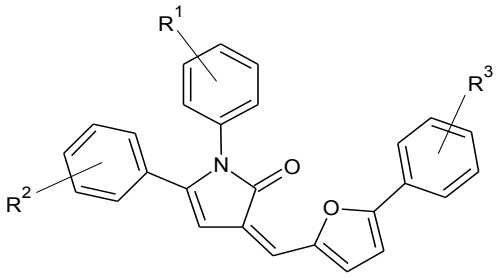

Figure7. Pyrrolinonesof general structure.

2.1.1. Niemann-Pick C1 Like 1 (NPC1L1)

Niemann-Pick C1 like 1 (*Npc1l1*) gene was initially identified to be a homolog of *Npc1* and was predicted to be involved in intracellular cholesterol trafficking based on the fact that mutations in the *Npc1* gene result in a lipid storage disease, NPC1 disease (Yu, *et al.*, 2006).

The NPC1L1 protein is predicted to have a typical signal peptide, 13 putative transmembrane domains, extensive potential N-linked glycosylation sites, and a conserved N-terminal "NPC1" domain. Interestingly, NPC1L1, like its homolog NPC1, also contains a sterol- sensing domain (SSD), a region conserved in at least six other polytopic membrane proteins, all of which are implicated in cholesterol metabolism, including 3-hydroxy-3-methylglutaryl-CoA reductase (HMGCR), the rate-limiting enzyme of cholesterol synthesis; and sterol regulatory element-binding protein cleavage-activating protein (SCAP), a protein that controls the transport and proteolytic activation of sterol regulatory element-binding proteins, which are membranebound transcription factors governing the synthesis of cholesterol and other lipids (Yu, *et al.*, 2006).

NPC1L1 protein is widely expressed in many human tissues, with the highest expression in the liver and small intestine (Yu, et al., 2006). NPC1L1 protein has been established as a primary regulator for intestinal cholesterol absorption and whole body cholesterol homeostasis (Howell, *et al.*, 2010).

An analysis of cellular mechanisms related to cellular cholesterol homeostasis shows that a decrease in cholesterol content within the LSOs can be explained by one or a combination of the following mechanisms: (1) increase in the cholesterol efflux from the LSOs; (2) decrease in the uptake of cholesterol; (3) decrease in the hydrolysis of cholesteryl esters by LAL (Rosenbaum, *et al.*, 2010).

Considering on the second mechanism to execute might have reasonable two options: (1) decreasing absorbed cholesterol level by inhibition of NPC1L1; (2) down-regulating NPC1L1 gene expression.

2.1.1.1. Decreasing absorbed cholesterol level by inhibition of NPC1L1

Ezetimibe (Fig.8) a cholesterol-absorption inhibitor (CAI) approved by FDA for the treatment of hypercholesterolemia (Howell, *et al.*, 2010). Along with statins, which lower LDL cholesterol levels by inhibition of cholesterol biosynthesis mediated by HMGCR, the cholesterol absorption inhibitor ezetimibe has been

shown to be effective in decreasing blood LDL cholesterol levels by decreasing uptake of dietary cholesterol (McMasters, *et al.*, 2009).

Ezetimibe was discovered using an empirical, *in vivo* screening protocol. It was later determined that ezetimibe inhibits intestinal cholesterol absorption by binding to NPC1L1 and recently two residues on loop C of NPC1L1 were shown to be important for ezetimibe binding. The development of an *in vitro* binding assay has considerably increased the capacity for testing compounds, suggesting the possibility of identifying structurally novel NPC1L1 inhibitors (McMasters, *et al.*, 2009).

Ezetimibe is a 2-azetidinone with three distal aryl rings-one phenol and two p-fluoro-phenyl groups. *In vivo*, the phenol undergoes glucuronidation to yield the more potent NPC1L1 inhibitor ezetimibe–glucuronide (Fig.8) (McMasters, *et al.*, 2009).

Researchers (McMasters,*et al.*, 2009) were interested in pursuing chemical scaffolds other than that of ezetimibe. Although slight modifications to the 2-azetidinone core have been reported, they were interested in finding a more diverse set of new chemical scaffolds and discovered a series of spiroimidazolidinone NPC1L1 inhibitors.

Pfefferkorn *et al.* (2008) have been interested in replacement of the β-lactam core of ezetimibe with alternative heterocycles. They reported the design and evaluation of a series of substituted oxazolidinones as ligands for NPC1L1 protein, a key mediator of cholesterol transport.

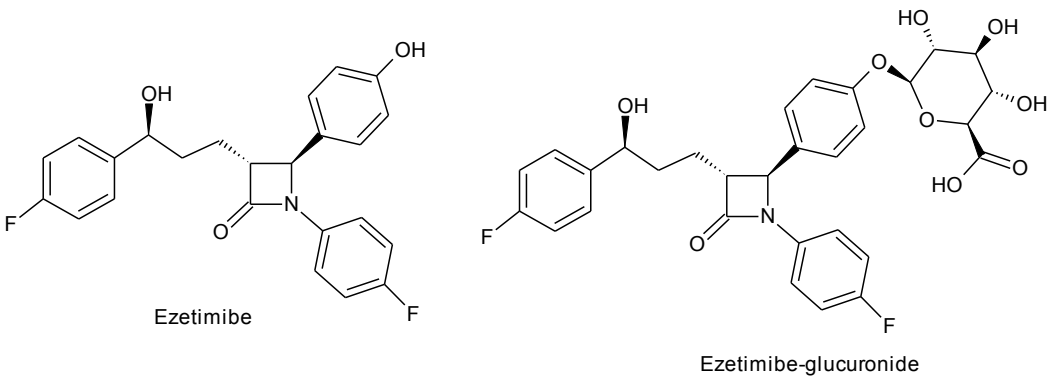

Figure 8. Structures of ezetimibe and ezetimibe–glucuronid.

2.1.1.2. Down-regulating NPC1L1 gene expression

Valasek *et al.* (2007) hypothesized that fenofibrate might modulate NPC1L1 expression to alter intestinal cholesterol transport. They found that fenofibrate-treated wild-type mice have decreased fractional cholesterol absorption (35–47% decrease) and increased fecal neutral sterol excretion (51–83% increase), which correspond to decreased expression of NPC1L1 mRNA and protein (38–66% decrease) in the proximal small intestine.

Fenofibrate is known to bind PPARα to enhance fatty acid oxidation and decrease serum triglycerides in patients and can also decrease plasma total cholesterol and LDL-cholesterol levels while increasing high density lipoptotein (HDL)-cholesterol levels. Also, clofibrate and gemfibrozil can reduce cholesterol absorption efficiency in humans. Using the mouse model, they have delineated a molecular mechanism by which specific activation of PPARα by fenofibrate decreases cholesterol absorption via an inhibitory effect on NPC1L1 expression in the proximal small intestine (Valasek, *et al.*, 2007).

Veen *et al.* (2005) demonstrated that PPARβ/δ activation clearly reduced intestinal expression of NPC1L1, predominantly in the jejunal part of the small intestine, where most of the cholesterol absorption takes place.

Activations of PPARα and PPARβ/δ have been shown to down-regulate NPC1L1 gene expression *in vitro* both in human and mouse models (Iwayanagi, *et al.*, 2011).

In the present study, this second option is evaluated and studied on PPARs agonists for exploring a possible treatment NPC disease.

PEROXIME PROLIFERATOR-ACTIVATED RECCEPTORS (PPARs)

The Peroxisome Proliferator Activated Receptors (PPARs) are members of the nuclear receptor superfamily of ligand-activated transcription factors that regulate the expression of genes involved in fatty acid uptake and oxidation, lipid metabolism and inflammation (Coll, *et al.*, 2009). The three subtypes of PPARs designated as α, δ and γ (Fig. 9.a) bind to fatty acids and fatty acid metabolites

and regulate the expression of genes involved in the transport, metabolism and buffering of these ligands within cells. In rats, PPARα is most highly expressed in brown adipose tissue, followed by liver, kidney, heart and skeletal muscle (Kersten and Wahli, 2000). PPARγis most highly expressed in white and brown adipose tissue, but is also expressed in muscle, colon and liver. PPARβ/δ is expressed in all tissues studied to date (Shearer and Hoekstra, 2003).

To be transcriptionally active, PPARs need to heterodimerize with the 9-*cis* retinoic acid receptor (RXR) (NR2B). PPAR-RXR heterodimers bind to DNA-specific sequences called peroxisome proliferator-response elements (PPREs), consisting of an imperfect direct repeat of the consensus binding site for nuclear hormone receptors (AGGTCA) separated by one nucleotide (DR-1). These sequences have been characterized within the promoter regions of PPAR target genes (Fig. 9.c) (Coll, *et al.*, 2009).

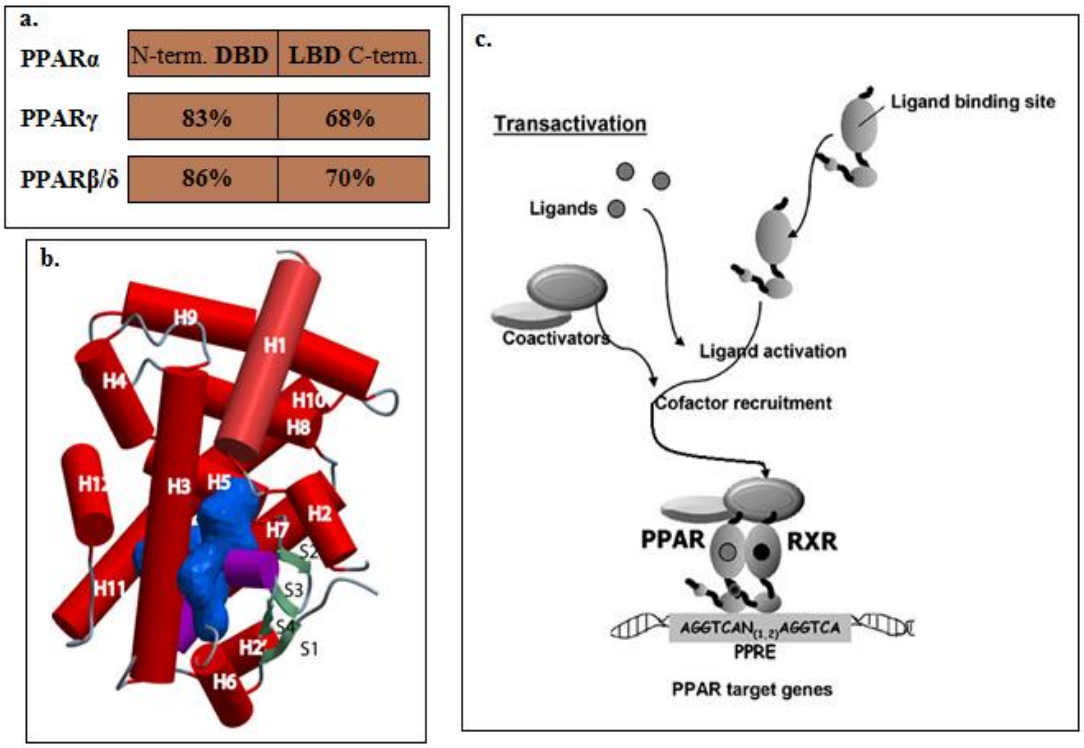

Figure 9. Quantities of domains, structure and binding model of PPARs. **a.** Indicated percent identities are for the human subtypes as compared to PPARα (Shearer and Hoekstra, 2003). **b.** Structure of PPAR. **c.** Following binding of a ligand, the PPAR/RXR heterodimer binds to a DR-1 response element in the regulatory regions of target genes. Agonist binding to the heterodimer leads to transcriptional activation (Coll, *et al.*, 2009).

1. PPARα

PPARα acts as a ligand-activated transcription factor in response to a variety of fatty acids. Fibrates, including fenofibrate, exert their biological effects by binding PPARα. As such, PPARα regulates the expression of genes involved in lipid metabolism, especially fatty acid oxidation and transport. Treatment with PPARα agonists enhances fatty acid oxidation, decreases plasma triglycerides, and may promote reverse cholesterol transport (Valasek, *et al.*, 2007).

Although the PPARα DBDs are identical across a variety of species, the LBDs exhibit lower homology, possibly reflecting evolutionary adaptation to different dietary ligands. A comparison of human PPARα to its murine counterpart reveals an 85% identity at the nucleotide level and a 91% identity at the amino acid level (Willson, *et al.*, 2000).

1.1. PPARαLigands

PPARα binds to a diverse set of ligands, like arachidonic acid metabolites (prostaglandins and leukotrienes) and plasticizers and synthetic fibrate drugs, including clofibrate, fenofibrate and bezafibrate (Fig.10). Given that no single high affinity natural ligand has been identified for PPARα, it has been proposed that a physiological role of the receptor may be to sense the total flux of dietary fatty acids in key tissues. Many PPARα ligands, including most of the common fibrate ligands, show only modest selectivity over the other PPAR subtypes. However, a potent thioisobutyric acid GW7647 (Fig.8) has been identified that shows excellent selectivity for both murine and human PPARα (Jackson, *et al.*, 1997), (Xu, *et al.*, 2002).

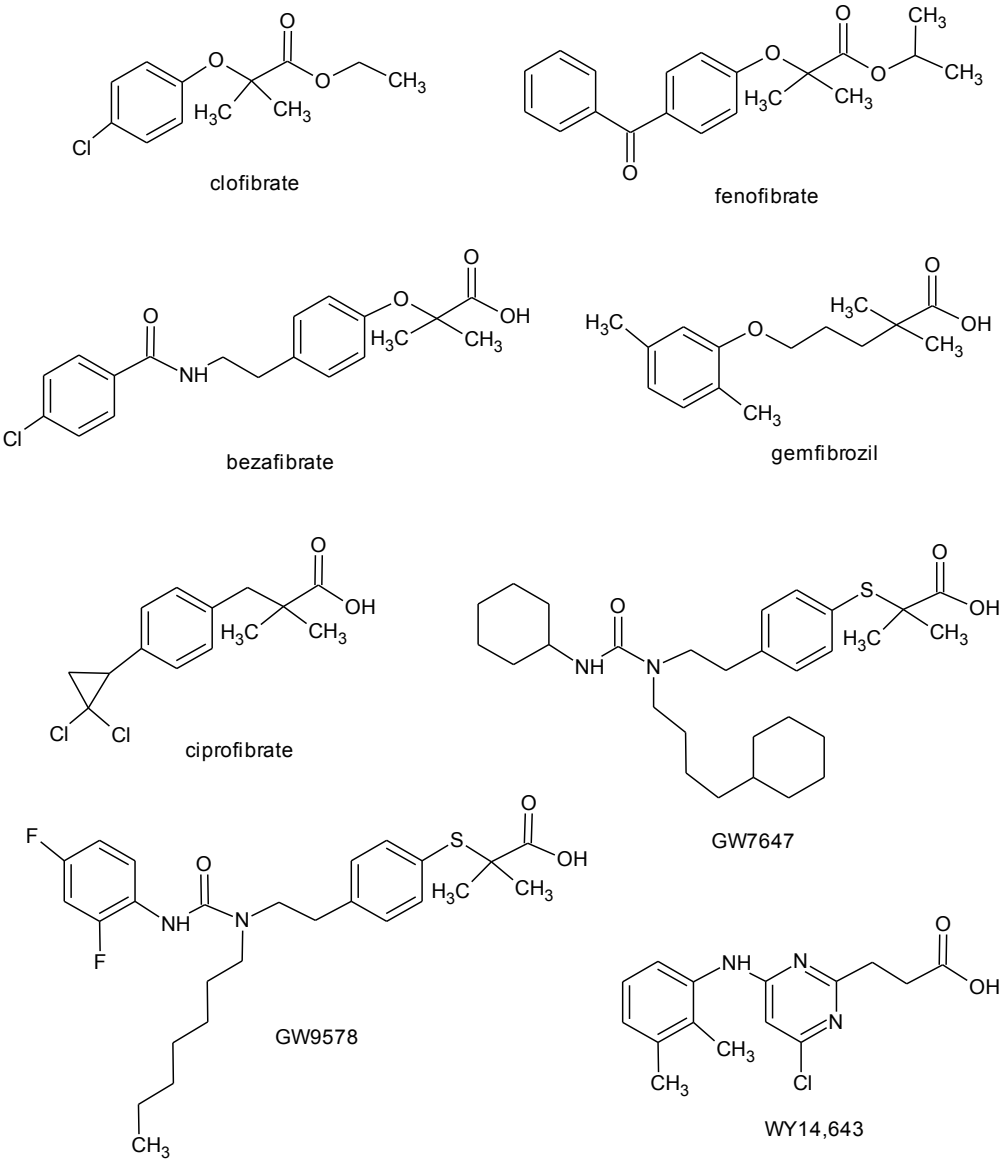

Figure 10. Structures of the PPARα Agonists (Shearer and Hoekstra, 2003).

2. PPARβ/δ

PPARβ/δ is involved in regulation of energy homeostasis. Activation of PPARβ/δ markedly increases fecal neutral sterol secretion, the last step in reverse cholesterol transport. This phenomenon can neither be explained by increased hepatobiliary cholesterol secretion, nor by reduced cholesterol absorption. To test the hypothesis that PPARβ/δ activation leads to stimulation of transintestinal cholesterol efflux (TICE), we quantified it by intestine perfusions in FVB (friend

virus B) mice treated with PPARβ/δ agonist GW610742 (Fig. 11). To exclude the effects on cholesterol absorption, mice were also treated with cholesterol absorption inhibitor ezetimibe or ezetimibe/GW610742. GW601742 treatment had little effect on plasma lipid levels but stimulated both fecal neutral sterol excretion (200%) and TICE (100%). GW610742 decreased intestinal NPC1L1 expression. Although treatment with ezetimibe alone had no effect on TICE, it reduced the effect of GW610742 on TICE. These data show that activation of PPARβ/δ stimulates fecal cholesterol excretion in mice, primarily by the two-fold increase in TICE (Vrins, *et al.*, 2009).

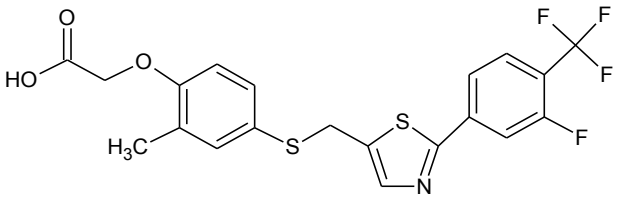

GW610742

Figure 11. Chemical structure of the PPARβ/δ-specific agonist GW610742 (Veen, 2005).

3. PPARγ

PPARγ has been the most extensively studied PPAR subtype to date. Two distinct N-terminal isoforms, termed PPARγ1 and PPARγ2, have been identified in mice and humans (Mukherjee, *et al.*, 1997). PPARγ is a pivotal transcription factor in the regulation of adipocyte gene expression and differentiation. The regulation of adipocyte differentiation by PPARγ takes place through a coordinated signaling cascade involving other families of transcription factors and has been reviewed (Spiegelman, *et al.*, 1996).In addition to adipogenic effects, PPARγ has been shown to be an important regulator of target genes involved in glucose and lipid metabolism. PPARγagonists are efficacious antidiabetic agents and represent a novel class of successfully marketed diabetes drugs (Willson, *et al.*, 2000).

3.1. PPARγLigands

3.1.1. Natural Ligands

While significant debate continues over the identity of the natural ligand(s) for PPARγ, studies have shown numerous naturally occurring fatty acids, eicosanoids, prostaglandins and their metabolites to be weak endogenous activators of PPARγ. PPARγ exhibits modest preference for essential polyunsaturated fatty acids (PUFAs) including linoleic acid, linolenic acid, arachidonic acid and eicosapentaenoic acid. Certain oxidized metabolites of PUFAs such as 9- or 13-hydroxyoctadecadienoic acid (9-HODE or 13-HODE) and 15-deoxy-12,14-prostaglandin J2 (15d-PGJ2), have been demonstrated to result in increased PPARγ-mediated transactivation (Nagy, *et al.*, 1998), (Hulin, *et al.*, 1996). Thus, PPARγ may serve as a generalized fatty acid sensor that couples changes in overall PUFA concentrations with the target genes associated with lipid and glucose homeostasis (Shearer and Hoekstra, 2003).

3.1.2. Synthetic Agonists

The thiazolidinedione (TZD) class of antidiabetic agents, commonly referred to as "glitazones", represent the first compounds identified as high affinity PPARγ agonists (Buckle, *et al.*, 1996). Two glitazones, rosiglitazone (Avandia) and pioglitazone (Actos) are currently marketed for the treatment of type 2 diabetes (Fig.10). Troglitazone (Rezulin), a third approved glitazone, was withdrawn from the marketplace due to liver toxicity (Fig.12) (Shearer and Hoekstra, 2003).

A series of PPARγ agonists, exemplified by GI262570 (Farglitazar), GW1929 and GW7845, have also been developed (Henke, *et al.*, 1998), (Collins, *et al.*, 1998), (Cobb, *et al.*, 1998) (Fig.12). These compounds represent the first antidiabetic agents to be optimized based upon their activity on human PPARγ. This class of PPARγ agonists also represents some of the most potent agonists reported to date. The (*S*)-enantiomers have been shown to possess greater binding affinity and

functional activity at PPARγ than the corresponding (*R*)-enantiomers (Collins, *et al.*, 1998). In cell based transactivation assays, these analogs exhibit up to 1000-fold selectivity for PPARγ over the PPARα and PPARδ subtypes (Collins, et al., 1998), (Cobb, *et al.*, 1998) (Fiedorek, *et al.*, 2000). Farglitazar has shown potent reduction of glucose activity, reduction of triglycerides and elevation of HDL cholesterol in diabetic patients in Phase II studies (Fiedorek, *et al.*, 2000), (Wilson, *et al.*, 2000). The positive lipid effects of farglitazar may be due to residual PPARα activity in the compound (Shearer and Hoekstra, 2003).

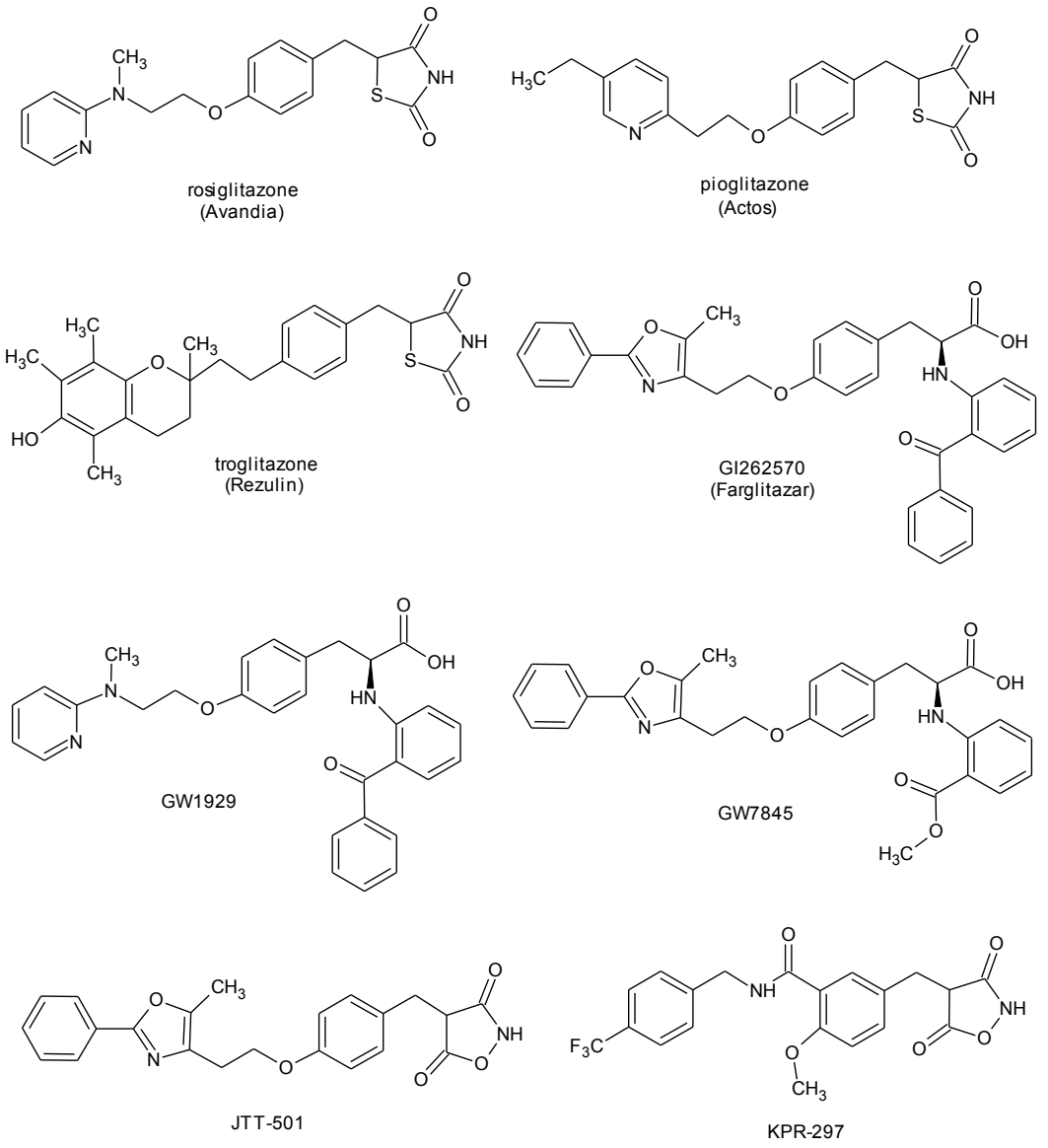

Figure 12. Structures of the PPARγ Agonists (Shearer and Hoekstra, 2003).

4. Aims of the Research

Structures of the LBD of the PPARs in the absence and presence of ligands have been solved by X-Ray crystallography (Gampe, *et al.*, 2000), (Nolte, et al., 1998), (Uppenberg, *et al.*, 1998), (Willson, *et al.*, 2001), (Xu, *et al.*, 1999), (Xu, *et al.*, 2001), (Xu, *et al.*, 2002). The apo-PPARγ LBD crystal structure shows the receptor consists of a bundle of 13 α-helices and a small four-stranded β-sheet arranged in a canonical helical sandwich fold commonly observed for other nuclear receptors (Nolte, *et al.*, 1998). Each of the PPAR subtypes possesses a similar Y-shaped binding pocket located within the lower half of the LBD that extends from the C-terminal AF-2 helix to the β-sheet between helices H3 and H6. However, marked differences in the detailed topology of the binding pockets allow for selective ligand binding. The solved structures for ligand-bound PPARs reveal that agonists, such as TZDs, fibrates and fatty acids, share a common binding mode in which their acidic head groups participate in an intricate hydrogen bonding network within the ligand binding pocket that includes a key tyrosine residue located in the C-terminal AF-2 helix. These interactions form a charge clamp that effectively stabilizes the receptor into a conformation permissive to the recruitment of co-activator proteins, such as SRC-1 required for transcriptional activation (Nolte, *et al.*, 1998), (Uppenberg, *et al.*, 1998), (Gampe, *et al.*, 2000).The receptor adopts a conformation similar to the apo-PPARγ with GW0072 occupying the ligand binding pocket in a region distal from the residues involved in agonist stabilization of the AF-2 helix. In this structure, the charge clamp is not stabilized by the ligand which may account for its weak agonist activity (Shearer and Hoekstra, 2003).

X-Ray crystallography studies about molecular dynamic and studies in silico, using the most recent technologies have been more interesting to evaluate biological activities of PPARs ligands and to search and find new molecules that can be used as innovative molecules which response better than the old ones at the toxicological profile. Recently, have been find novel structural models able to interact whit PPARs' action site in order to give a biological response both of *in vitro* and *in vivo*. Recently, X-Ray studies on molecular complexes have shown

that there are new ways of interaction about receptor and ligand and this is an innovative aspect of partial agonism of some ligands and their receptors. This characteristic could be used to make powerful therapeutic aspects of these molecules and weak collateral effects.

In the previous studies, synthesis and biological evaluation of some compounds activity on PPARα and PPARγ, which were structurally-like to clofibric acid had been studied (Fig.13) (Carrieri, *et al.*, 2013).

To evaluate biological activity WY14,643 was used like reference for PPARα and Rosiglitazone for PPARγ, using transactivation assay on cellular lines.

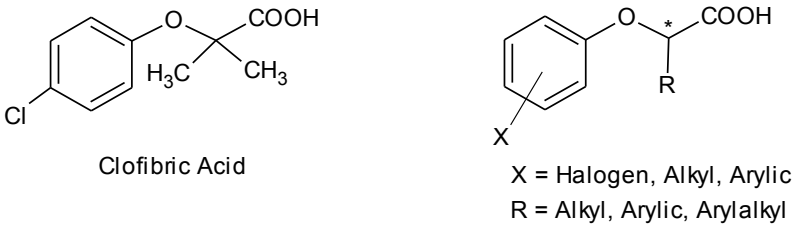

Figure 13. Structures of clofibric acid derivatives.

Results they had during these years, gave information about structure-activity relationships (SARs) of these compounds on PPARs:

- Compounds synthesized and tested were truly agonists on PPARα and were more powerful than clofobric acid and WY14,643.
- Chains longer or benzylic substituents on chiral center improve biological activity on both receptors studied.
- Absolute configuration played an important role when on the chiral carbon in α to the carboxylic group there is an n-propyl, a phenyl or benzyl group; in particular, enantiomer (*S*) is more important than enantiomer (*R*).
- All of the synthesized compounds for PPARγ had less activity than Rosiglitazone.

In the Table 2, there are the two compounds which had the best pharmacological profile. These two compounds have absolutely configuration (*S*) and they show activity on both receptors.

	PPARα		**PPARγ**	
Compound	EC_{50} (μM)	Efficacy (%)	EC_{50} (μM)	Efficacy (%)
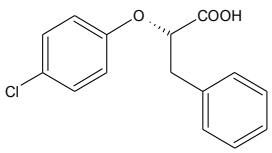	3.9	99.4	2.7	58.8
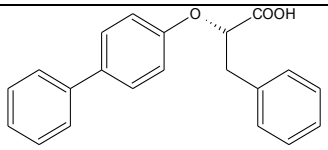	0.5	124.2	0.5	91.8
WY14,643	1.6	100	-	-
Rosiglitazone	-	-	0.039	100

Table 2. Activity of PPAR Agonists in Cell-Based Transactivation Assays (Carrieri, *et al.*, 2013)

With the aims to identify novel structures having a new scaffold not very similar to other PPARs agonists, *virtual screening* was performed on a big number of new compounds to find some that could have biological activity. Thanks to the progress of the molecular pharmacology and according to molecular-receptor interaction simulation, it was possible to use molecules to find novel lead compounds. This way, known as Molecular Modeling, is able to foresee the arrangement of the receptor and the structure of the compound. In this way it is possible to elaborate a novel compound based on its receptor structure target, its chemical composition and its spatial orientation.

Structural information about PPARs binding pocket bring to project and synthesis of compound AL26-18 (Fig. 14), born by Professor Antonio Lavecchia's studies, who works at the Department of Pharmacy of the University of Naples. According

to data tests this structure has a good activity on PPARα and PPARγ and shows activity on PPARβ/δ, too. So, this structure is pan-agonist and in particular, it is full agonist for PPARα and partial agonists for PPARγ, and its' derivatives are active on PPARβ/δ, too. Because of the great importance that the concept of isosterism and structural modification of the lead compound, have in the field of medicinal chemistry, our attention has been focused on the modification of its structure in the aromatic portion and in the synthesis of isosters of the parent molecule. In this study, compounds, as shown in Figure 15, have synthesized and hypothesized to give a good activity on both receptors, taking place on the binding pocket. After, these compounds were tested to evaluate their biological activities using PPARs transfection assay. This methodology is the most used in the modulation of molecular. The basic concept of the method is to introduce modifications in the reference molecule such that, while varying some structural characteristics and physicochemical, will maintain intact the possibility to recognize the same receptor. In other words, two isosteric molecules must submit, within certain limits, the same shape and the same volume. All of the information that collecting from all the structural variations determine the SARs which permit the identification of pharmacophore and are the basis for further molecular manipulations.

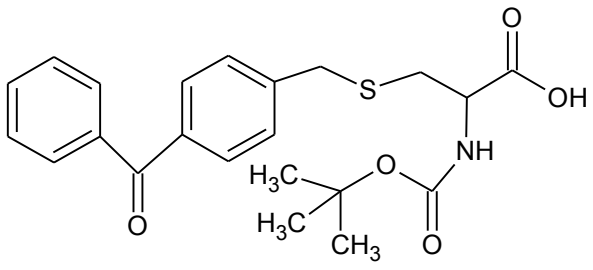

AL26-18

Figure 14. Chemical structure of AL26-18 (**Compound 1**).

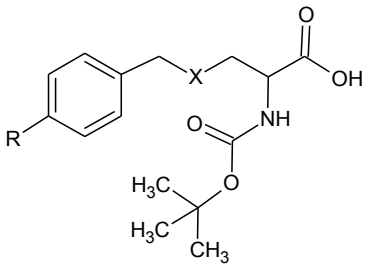

Comp. 1. (*R,S*) R=PhCO, X=S
Comp. 2. (*R,S*) R=PhCO, X=O
Comp. 3. (*R,S*) R=PhCH$_2$, X=S
Comp. 4. (*R,S*) R=PhCH$_2$, X=O
Comp. 5. (*R,S*) R=Ph, X=S
Comp. 6. (*R,S*) R=Ph, X=O

Comp. 1a. (*R*) R=PhCO, X=S
Comp. 2a. (*R*) R=PhCO, X=O

Comp. 5a. (*R*) R=Ph, X=S

Figure 15. Structural modification and isosteres.

MATERIALS AND METHODS

1. Materials

Reaction was followed on TLC using Thin Layer on silica gel 60 F254 (Merck). Retention Factors were calculated using different mixture of solvent like eluents. To see compounds on TLC UV lamp is used.

Chromatography was performed on silica gel 60 Merck (40-60μm). The crude was dissolved on the same eluent we used to separate the mixture.

Mass analyses were performed on Agilent 6890N-5973N GC-MSD e Agilent 1100 Series LC-MSD Trap System VL.

^{1}H-NMR analyses were performed on Varian-Mercury 300 (chemical shift expressed in δ).

Melting points were performed on Melting Point Apparatus Gallenkamp.

The polarimetric measurements were performed with a Perkin-Elmer model 341 polarimeter, using a cell with an optical path of 10 cm, at the wavelength of the sodium D line (589 nm), at a temperature of 20 °C. The solutions were prepared dissolving 20 mg of substance in 2mLof methanol.

Mass spectra were recorded on an HP GC/MS 6890-5973 MSD spectrometer, electron impact 70 eV, equipped with HP chemstation or an Agilent LC/MS 1100 Series LC/MSD Trap System VL spectrometer, electrospray ionization (ESI).

The enantiomeric excesses of acids were determined by HPLC analysis of acids on Chiralcel OD or AD columns (4.6 mm i.d. × 250 mm, Daicel Chemical Industries, Ltd, Tokyo, Japan).

Analytical liquid chromatography was performed on a PE chromatograph equipped with a Rheodyne 7725i model injector, a 785A model UV/vis detector, a series 200 model pump and NCI 900 model interface.

All solvent and all reactant, commercial available, used in reactions and preparation of samples for analysis were bought from Sigma Aldrich, Fulcra and Lancaster.

2. Experimental Procedures

Figure 16 shows the synthesis of **Comp. 1**, **2**, **2a**, **3**, **4** and **6**. The 4-(bromomethyl)benzophenone, commercially available, or 1-benzyl-4-(bromomethyl)benzene, is synthesized, are reacted with *N*-(*tert*-butoxycarbonyl)-(*L*)-serine, is also commercially available, *N*-(*tert*-butoxycarbonyl)–(*L*)–cysteine, *N*-(*tert*-butoxycarbonyl)-(*D,L*)-serine or with *N*-(*tert*-butoxycarbonyl)-(*D,L*)-cysteine, are synthesized, in nitrogen atmosphere and in the presence of NaH, using DMF dry as the solvent. The acid **(A)** that is obtained is reacted with benzylamine or cyclohexylamine to give the corresponding salt **(B)** in which it is still present in the *tert*-butoxycarbonyl (*t*-Boc) protection of the amino group, as demonstrated by singlet at 1.41 ppm in the ^{1}H-NMR spectrum relative to the three CH_3 of the *tert*-butoxy group. $[\alpha]_D$ values show optical rotation of -23.7 for the cyclohexylamine salt of the **Comp. 2a**, a result that confirms the value of $[\alpha]_D$ found also with the other route of synthesis. The value of E.E.is 82%.

Figure 17 shows the synthesis of **Comp. 5** and both **Comp. 1a** and **5a** in absolute configuration (*R*). The 4-(bromomethyl)biphenyl or 4-(bromomethyl) benzophenone, both commercially available, is reacted with the (R)-2-*tert*-butoxycarbonylamino-3-mercapto-propionic acid methyl ester, commercially available, in DMF in the presence of Cs_2CO_3 until complete disappearance of the

starting reagents. Compound **(C)** is subsequently hydrolyzed in basic conditions, using 1N LiOH in the presence of THF to give the corresponding acid **(D)** in which is still present in the *t*-Boc protection of the amino group, as shown by the singlet to 1.46 ppm in the ^{1}H-NMR spectrum. A part of compound **(D)**, purified by crystallization $CHCl_3$/n-Hexane. Optical purity by HPLC and optical rotation were evaluated for obtained products. **Comp. 1a** and **5a** were synthesized in optically active form, it was necessary to use HPLC. They have presented the values of $[\alpha]_D$ and E.E. +2, 97% and -29, 91% respectively, **Comp. 1a** and **5a**.

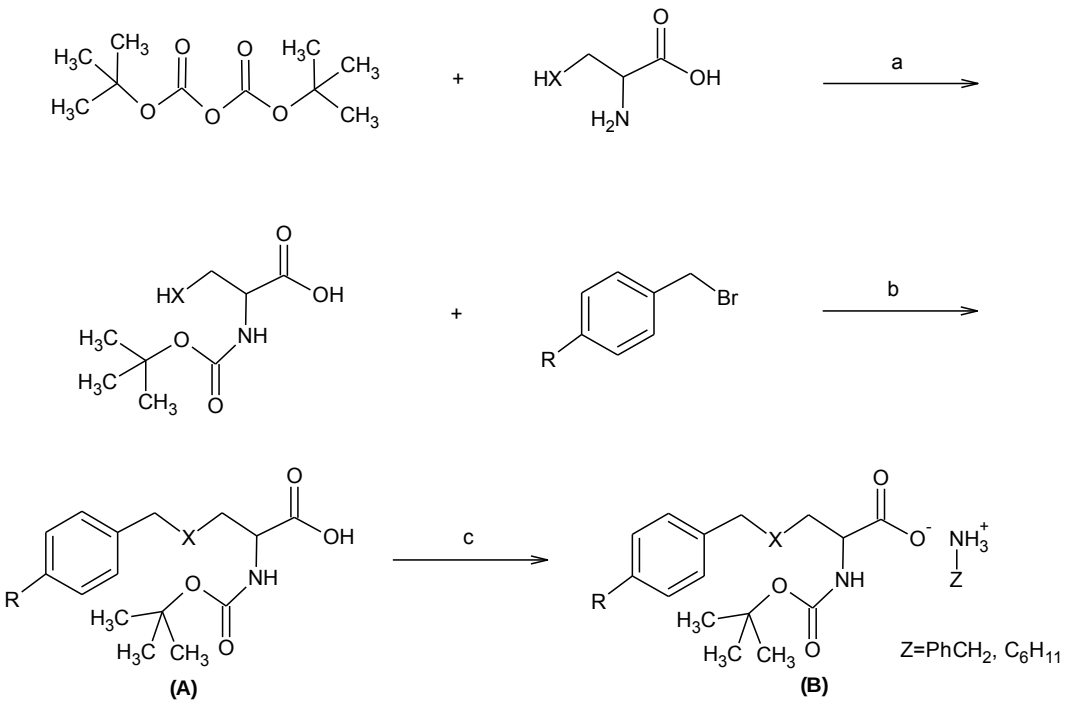

Comp. 1. (R,S) R=PhCO, X=S
Comp. 2. (R,S) R=PhCO, X=O
Comp. 3. (R,S) R=$PhCH_2$, X=S
Comp. 4. (R,S) R=$PhCH_2$, X=O
Comp. 6. (R,S) R=Ph, X=O

Comp. 2a. (R) R=PhCO, X=O

a. Acetone, NaOH, 0°C , R.T, 4h.
b. NaH, DMF dry, N_2, 0 °C , R.T, 24h.
c. Benzylamine or Cyclohexylamine (1:1), Et$_2$O
d. TES, CF_3COOH, Cromatography on silica gel Hex/EtOAc; 99.5:0.5-99:1

Figure 16. General synthesis route of **Comp. 1**, **2**, **2a**, **3**, **4** and **6**.

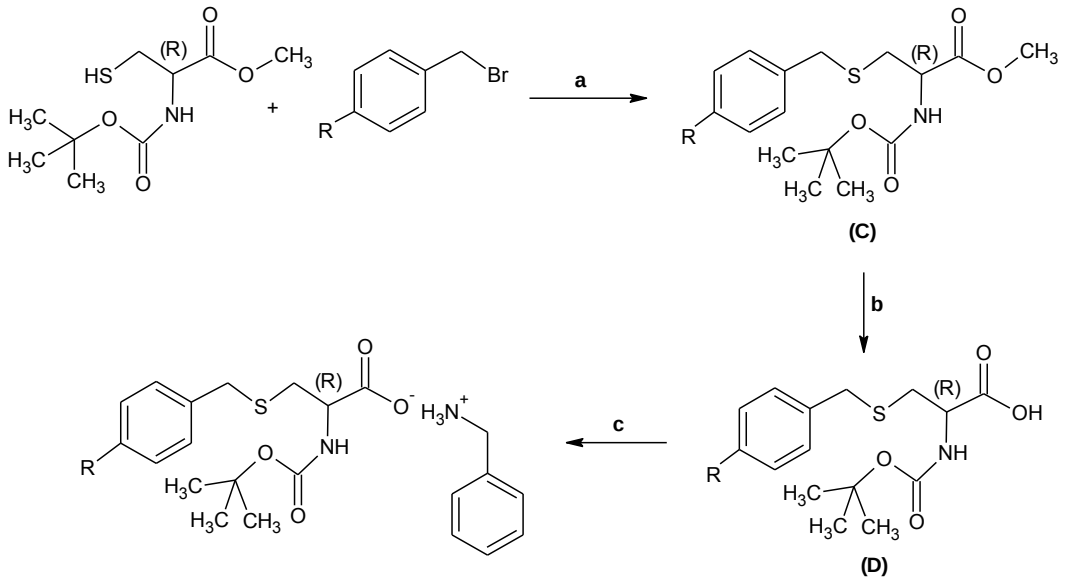

Comp. 5. R=Ph, X=S

Comp. 1a. R=PhCO, X=S
Comp. 5a. R=Ph, X=S

a. Cs_2CO_3, DMF, RT, 5h., Chromotography on silica jel Hex/EtOAc; 7:3

b. LiOH 1N, THF (1:1), RT, overnight

c. Benzylamine (1:1), Et_2O

Figure 17. General synthesis route of **Comp. 1a**, **5** and **5a**.

2.1. Synthetic Route of Compound 1

2.1.1. (*D,L*)-2-*tert*-Butoxycarbonylamino-3-mercapto propionic acid

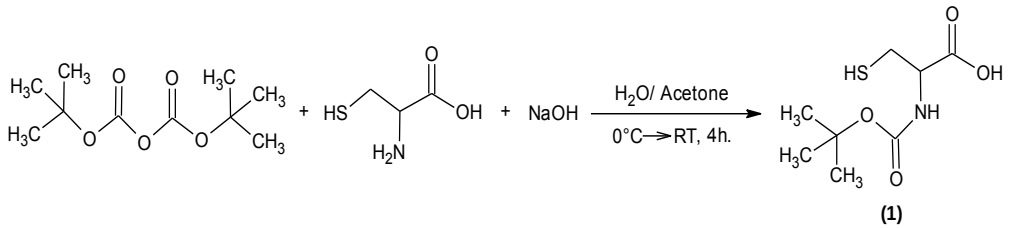

	Boc_2O	(*D,L*)-Cysteine	NaOH	H_2O/Acetone	*N*-Boc-(*D,L*)-Cysteine (1)
MW (g/mol)	281.21	121.16	40		221.28
mMol	25.50	24.76	28.50		10.62
m	7.170 g	3.00 g	1.140 g		2.350
SR	1	1			
Vol.				21 mL+12mL/ 16 mL	

(*D,L*)-Cysteine (3.00g; 24.76 mMol) was dissolved in distillated water (21 mL). A solution of NaOH (1.140 g/12 mLH_2O) was added and the reaction was stirred at 0°C before to add a solution of Boc_2O (7.170 g, 25.50 mMol/16 mL Acetone).The reaction was stirred at room temperature for 4 hours. Solvent was evaporated and citric acid 10% was added arriving to pH 3. The water phase was extracted three times using EtOAc. The organic phase was washed with water, brine, dried over Na_2SO_4, filtered on cotton and evaporated in vacuum to have white solid that is purified by crystallization using only $CHCl_3$ (2.350 g; 10.62 mMol; yield: 43%).

^{1}H-NMR (300 MHz, $CDCl_3$, δ): 1.46 (s, 9H) (*CH_3)$_3$*C-; 2.91-3.07 (bb, 2H) SH*CH_2*CH-; 4.64-4.67 (b, 1H) CH_2*CH*COOH; 5.44 (d, 1H) CH*NH*CO-.

Melting Point: 130.4-134.8 °C

2.1.2. (*R,S*)-3-(4-Benzoyl-benzylsulfanyl)-2-*tert*-butoxycarbonylamino propionic acid

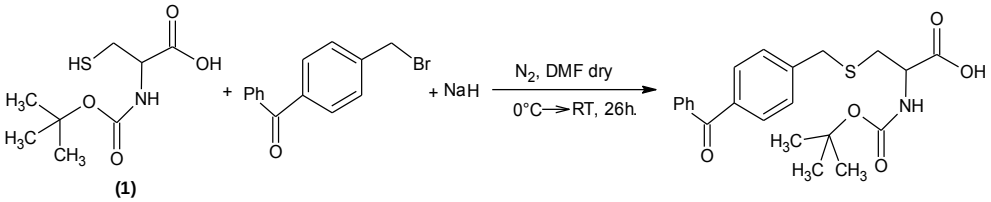

	N-Boc-(*D,L*)-Cysteine (1)	4-(Bromomethyl)benzophenone	NaH	DMF dry	Comp. 1
MW (g/mol)	221.28	275.14	24		415
mMol	0.90	0.85	4.17		1.23
m	0.200 g	0.235 g	0.100 g		0.510 g
SR	1	1			
Vol.				6 mL+3 mL	

In a double-necked flask, under nitrogen atmosphere, NaH (0.100 g; 4.17 mMol) was dissolved in DMF dry (6 mL). At 0 °C, *N*-Boc-(*D,L*)-cysteine (0.200 g; 1.90 mMol) was added. Then, a solution of 4-(bromomethyl)benzophenone (0.235 g; 0.85 mMol) in DMF dry (3 mL) was added drop wise. The reaction was stirred at room temperature for 26 hours. The reaction was quenched with ice and HCl 2N was added arriving to pH 2 (3 mL). The water phase was extracted for three times

using EtOAc (30 mL). The organic phase was washed with distillated water and brine, dried over Na_2SO_4, filtered on cotton and evaporated in vacuum to have yellow oil (0.510 g; 1.23 mMol).

2.1.3. (*R,S*)-3-(4-Benzoyl-benzylsulfanyl)-2-*tert*-butoxycarbonylamino propionic acidbenzylamine salt

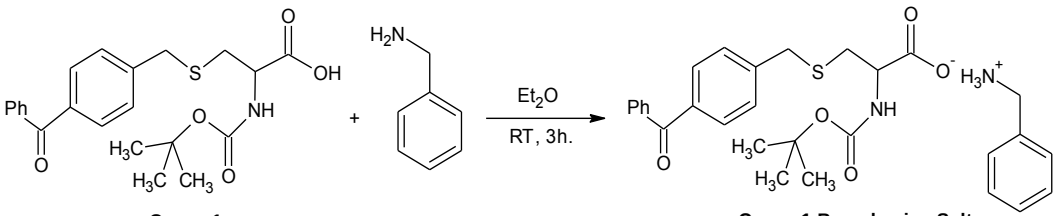

Comp. 1 **Comp. 1 Benzylamine Salt**

	Comp. 1	**Benzylamine**	**Et_2O**	**Comp. 1 Benzylamine Salt**
MW (g/mol)	415	107.15		522.63
mMol	1.23	1.63		0.48
m	0.510 g	0.175 g		0.250 g
Sr	1	1		
Vol.			20 mL	

The acid (0.510 g; 1.23 mMol) was dissolved in Et_2O (20 mL) and benzylamine (0.175 g; 1.63 mMol) was added. The reaction was stirred for 3 hours at room temperature. It was filtered on gooch to have white solid (0.250 g; 0.48 mMol; yield: 39%).

^{1}H-NMR (300 MHz, $CDCl_3$, δ):1.41 (s, 9H) $(CH_3)_3$C; 2.72-2.95 (bb, 2H) SCH_2CH; 3.72 (s, 2H) PhCH_2S; 3.95 (s, 2H) Ph$CH_2NH_3^+$; 4.15 (b, 1H) $CH_2CH$$COO^-$; 5.54 (b, 1H) CH*NH*- *t*-Boc; 7.28-7.76 (14H) aromatic protons.

HPLC: Sample conc.: 2 mg /mL EtOH 10 µL; column AD; mobile phase: Hex/*i*-PrOH/TFA 80:20:0.2; flow: 1 mL/min; l: 254 nm.

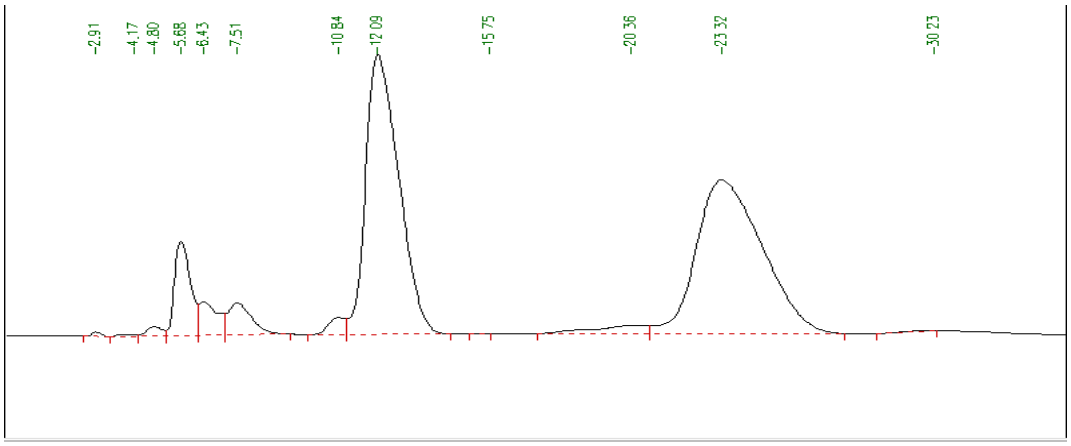

2.2. Synthetic Route of Compound 1a

2.2.1. (*R*)-3-(4-Benzoyl-benzylsulfanyl)-2-*tert*-butoxycarbonylamine propionic acid methyl ester

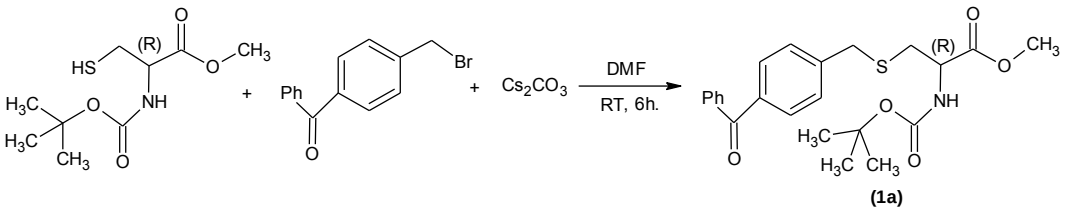

	N-Boc-*L*-Cysteine Methyl Ester	4-(Bromomethyl) biphenyl	Cs_2CO_3	DMF	(1a)
MW (g/mol)	235.30	275.14	325.82		429.55
mMol	2.12	2.04	4.26		1.20
m	0.500 g	0.560 g	1.389 g		0.517 g
SR	1	1			
Vol.				20 mL	

4-(Bromomethyl)benzophenone (0.560 g; 2.04 mMol) was dissolved in DMF (20 mL); Cs_2CO_3 (1.389 g; 4.26 mMol) and *N*-Boc-L-cysteine methyl ester (0.500 g; 2.12 mMol) were added to the solution. The reaction was stirred at room temperature for 6 hours and quenched adding 35 mL of distillated water. The water layer was extracted three times using EtOAc. The organic layer was washed

with brine, dried over Na_2SO_4, filtered on cotton and evaporated in vacuum, having yellow oil that is purified on silica gel (Hex/EtOAc; 7:3). It was yellow oil (0.517 g; 1.20 mMol; yield: 59%).

GC-MS (Relative Abundance %): 429 (0) $[C_{23}H_{27}NSO_5]$; 329 (18.5) $[C_{18}H_{18}NSO_3]^+$; 228 (16.1) $[C_{14}H_{12}SO]$; 196 (100) $[C_{14}H_{12}O]$; 167 (55) $[C_{12}H_7O]^+$; 105 (34.6) $[C_7H_5O]^+$; 77 (34.9) $[C_6H_5]^+$.

^{1}H-NMR (300 MHz $CDCl_3$, δ): 1.45 (s, 9H) $(CH_3)_3C$; 2.78-2.95 (bb, 2H) SCH_2CH; 3.75 (s, 3H) CH_3CO; 3.79 (s, 2H) $PhCH_2S$; 4.55 (b, 1H) CH_2CHCO; 5.29 (b, 1H) CHNHCO; 7.41-7.80 (9H) aromatic protons.

2.2.2. (*R*)-3-(4-Benzoyl-benzylsulfanyl)-2-*tert*-butoxycarbonylamino propionic acid

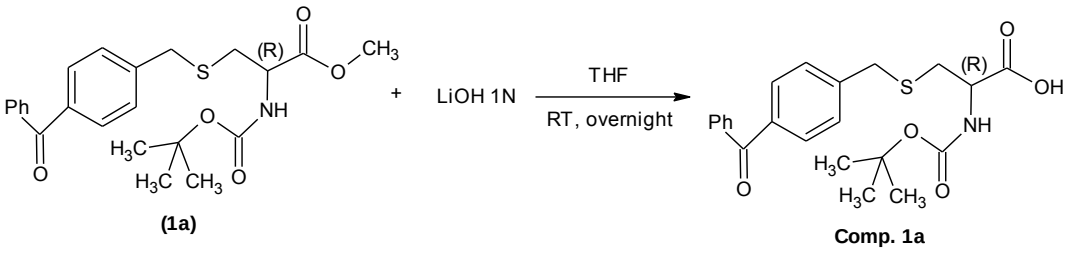

(1a) **Comp. 1a**

	(1a)	LiOH 1N	THF	Comp. 1a
MW (g/mol)	429.55			415.55
mMol	0.45			0.36
m	0.192 g			0.148 g
SR	1	1		
Vol.		3 mL	3 mL	

3-(4-Benzoyl-benzylsulfanyl)-2-*tert*-butoxycarbonylamino propionic acid methyl ester (0.192 g; 0.46 mMol) was dissolved in THF and LiOH 1N (3 mL) was added. The reaction was stirred overnight at room temperature. HCl 2N (1.5 mL) was added to the mixture and the water layer was extracted for three times with Et_2O. The organic layer was washed with brine, dried over Na_2SO_4, filtered on cotton and evaporated in vacuum, having brown oil. (0.148 g; 0.36 mMol; yield: 79%).

ESI-MS (Relative Abundance %): Negative: 414 (100) $[C_{22}H_{23}NSO_5]^+$; 340 (20)$[C_{16}H_{21}NSO_5]^+$; 296 (10) $[C_{17}H_{14}NSO_2]^+$; 227 (53) $[C_{14}H_{11}SO]^+$.

^{1}H-NMR (300 MHz $CDCl_3$, δ): 1.46 (s, 9H) $(CH_3)_3C$; 2.84-2.96 (bb, 2H) SCH_2CH; 3.81 (s, 2H) $PhCH_2S$; 4.54 (b, 1H) CH_2CHCO; 5.32 (b, 1H) $CHNHCO$; 7.42-7.80 (9H) aromatic protons.

2.2.3. (*R*)-3-(4-Benzoyl-benzylsulfanyl)-2-*tert*-butoxycarbonylamino propionic acid benzylamine salt

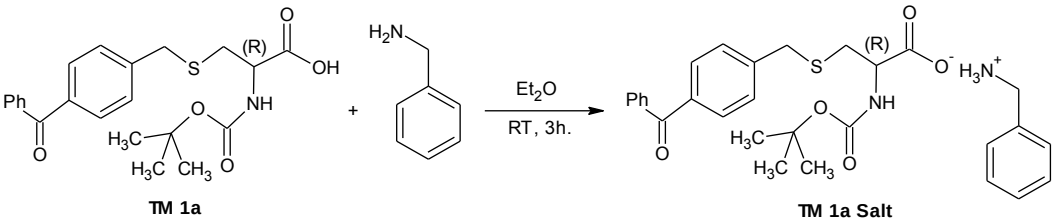

	Comp. 1a	Benzylamine	Et_2O	Comp. 1a Benzylamine Salt
MW (g/mol)	415.55	107.15		522.70
mMol	0.36	0.40		0.22
m	0.148 g	0.042 g		0.114 g
Sr	1	1		
Vol.			7 mL	

The acid (0.148 g; 0.36 mMol) was dissolved on Et_2O (7 mL) and a solution of benzylamine (0.042 g; 0.40 mMol) was added. The reaction was stirred for 3 hours at room temperature. A white solid was filtered (0.114 g; 0.22 mMol; yield: 61%).

ESI-MS (Relative Abundance %): Negative: 414 (79) $[C_{22}H_{24}NSO_5]^+$; 340 (27) $[C_{16}H_{21}NSO_5]$; 227 (100) $[C_{14}H_{11}SO]^+$. Positive: 523(23) $[C_{29}H_{33}N_2SO_5]^+$; 108 (31) $[C_7H_{10}N]$; 91(23) $[C_7H_7]^+$.

^{1}H-NMR (300 MHz $CDCl_3$, δ): 1.42 (s, 9H) $(CH_3)_3C$; 2.74-2.88 (bb, 2H) SCH_2CH; 3.73 (s, 2H) $PhCH_2S$; 3.98 (s, 2H) $PhCH_2NH_3^+$; 4.19 (b, 1H) CH_2CHCOO^-; 5.44 (b, 1H) CHNH- *t*-Boc; 7.30-7.77 (14H) aromatic protons.

Elementary Analysis: Calculated percentages: C: 66.64; H: 6.57; N: 5.36. Estimated percentages: C: 65.95; H: 6.42; N: 5.45.

[a]$_D$ **:**+2

HPLC: Sample conc.: 2 mg/mL EtOH, column AD; Hex/iPrOH/TFA 80:20:0.2; flow: 1 mL/min; l: 254 nm; injected vol.: 10 mL; retention time: 23.96'; ***E.E.: 97%***

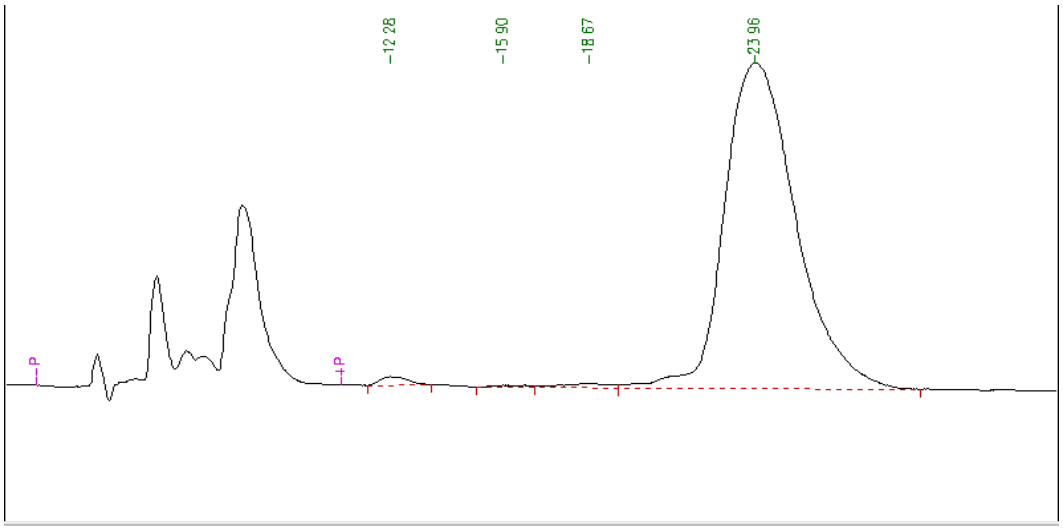

2.3. Synthetic Route of Compound 2

2.3.1. (*R,S*)-2-*tert*-Butoxycarbonylamino-3-hydroxy-propionic acid

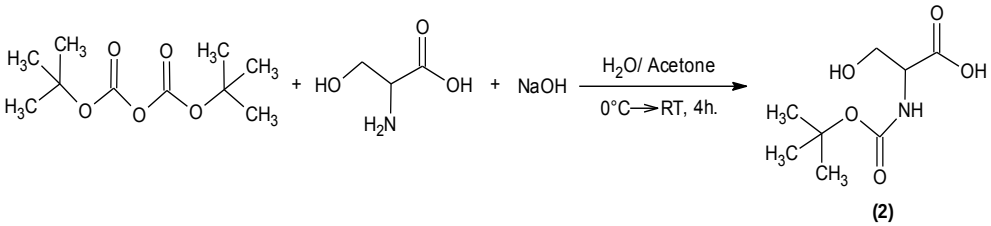

	Boc_2O	(*R,S*)-Serine	NaOH	H_2O/Acetone	*N*-Boc-(*R,S*)-Serine (2)
MW (g/mol)	281.21	105	40		205
mMol	52.32	50.01	50		33.74
m	11.2	5.255 g	2.00 g		6.916 g
SR	1	1			
Vol.				37 mL+21 mL/ 27 mL	

(*R,S*)-Serine (5.255 g; 50.01 mMol) was dissolved in distillated water (37 mL). A solution of NaOH (2.0 g/21 mL H_2O) was added and the reaction was stirred at 0 °C before to add a solution of Boc_2O (11.2 g; 52.32 mMol/27 mL Acetone). The

reaction was stirred at room temperature for 4 hours. Solvent was evaporated and citric acid 10% was added arriving to pH 3. The water phase was extracted three times using EtOAc. The organic phase was washed with water, brine, dried over Na_2SO_4, filtered on cotton and evaporated in vacuum to have transparent oil. (6.916 g; 33.74 mMol; yield: 67%)

ESI-MS (Relative Abundance %): Negative; 409 (8) $[2M-1]^+$; 204 (88) $[M-1]^+$; 130 (100) $[C_4H_6NO_4]$. Positive: 228 (100) $[M+Na]^+$; 172 (26) $[C_4H_6NO_5Na]^+$; 128(2) $[C_3H_6NO_3Na]^+$.

^{1}H-NMR (300MHz, $CDCl_3$, δ):1.40 (s, 9H) $(CH_3)_3$C-; 3.80-4.0 (bb, 2H) OHCH_2CH-; 4.27 (b, 1H) CH_2CHCOOH; 5.84 (b, 1H) CHNHCO-.

2.3.2. (*R,S*)-3-(4-Benzoyl-benzyloxy)-2-*tert*-butoxycarbonylamino propionic acid

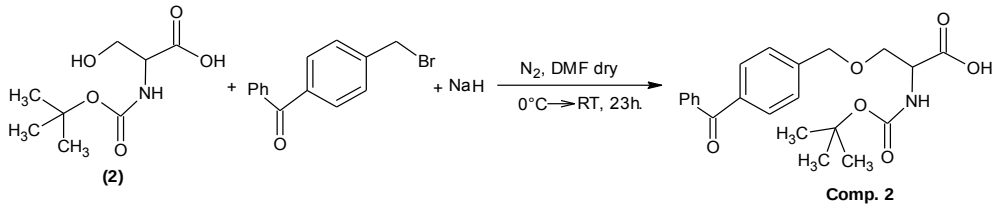

	N-Boc-(*R,S*)-Serine (2)	4-(Bromomethyl) benzophenone	NaH	DMF dry	Comp. 2
MW (g/mol)	205	275.14	24		399
mMol	1.91	1.82	9.08		1.88
m	0.596 g	0.500 g	0.218 g		0.752 g
SR	1	1			
Vol.				15mL+5mL	

In a double-necked flask, under nitrogen atmosphere, NaH (0.218 g; 9.08 mMol) was dissolved in DMF dry (15 mL). At 0°C, *N*-Boc-(*R,S)*-serine (0.596 g; 1.91 mMol) was added and a solution of 4-bromomethyl-benzophenone (0.140 g; 1.82 mMol) in DMF dry (5 mL) was added drop wise. The reaction was stirred at room temperature for 23 hours. The reaction was quenched with ice and HCl 2N was added arriving to pH 2 (5 mL). The water phase was extracted for three times using EtOAc (60 mL). The organic phase was washed with distillated water and

brine, dried over Na_2SO_4, filtered on cotton and evaporated in vacuum to have yellow oil (0.752 g; 1.88 mMol).

2.3.3. (*D,L*)-3-(4-Benzoyl-benzyloxy)-2-*tert*-butoxycarbonylaminopropionic acid cyclohexylamine salt

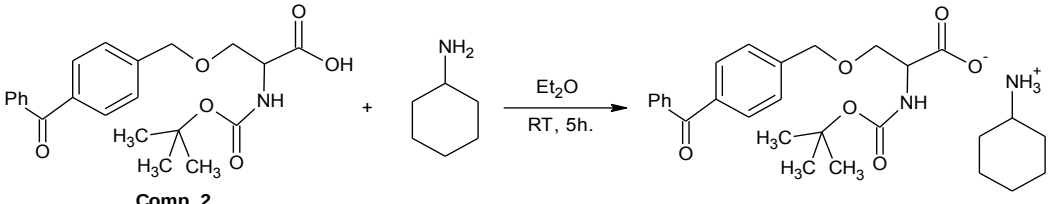

Comp. 2 — Comp. 2 Cyclohexylamine Salt

	Comp.2	Cyclohexyl-amine	Et_2O	Comp. 2 Cyclohexylamine Salt
MW (g/mol)	399	99		498
mMol	1.88	1.88		0.76
m	0.752 g	0.186 g		0.378 g
SR	1	1		
Vol.			52 mL	

The acid (0.752 g; 1.88 mMol) was dissolved in Et_2O (52 mL) and cyclohexylamine (0.186 g; 1.88 mMol) was added on. The reaction was stirred for 5 hours at room temperature. It was filtered on gooch to have white solid (0.378 g; 0.76 mMol; yield: 40%).

^{1}H-NMR (300 MHz, $CDCl_3$, δ): 1.42 (s, 9H) (CH_3)$_3$C; 1.16-2.95 (CH_2-Cyclohexylamine) 3.79-3.91 (dd, 2H) OCH_2CH; 4.41 (d, 1H) OCH$_2$*CH*; 4.60 (s, 2H) PhCH_2O; 5.56 (d, 1H) CH*NH*- *t*-Boc; 7.40-7.77 (9H) aromatic protons.

Elementary Analysis: Calculated percentages: 70.13% C; 7.93% H; 6.04% N. Estimated percentages: 60.97% C; 7.67% H; 6.95% N.

HPLC: Sample conc.: 3 mg/mL MeOH; injected vol.: 10 µL; column OD; mobile phase: Hex/*i*-PrOH/TFA 95/5/0.05; flow: 1 mL/min; detector: 230 nm; retention times: 24.03' and 27.88'

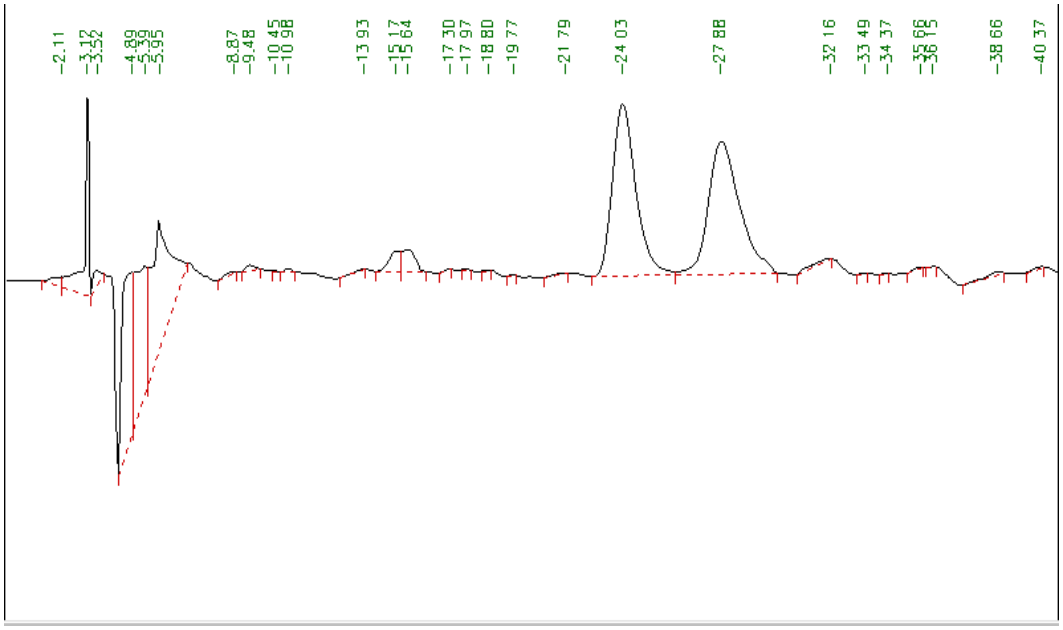

2.4. Synthetic Route of Compound 2a

2.4.1. (*R*)-3-(4-Benzoyl-benzyloxy)-2-*tert*-butoxycarbonylamino propionic acid

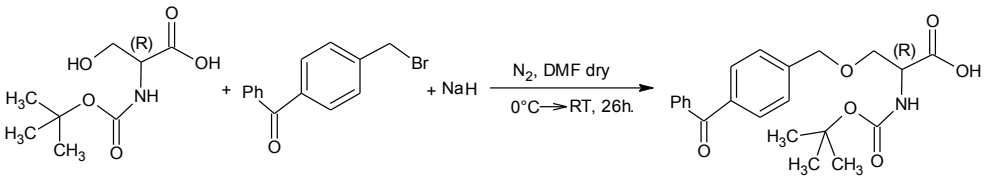

Comp. 2a

	N-Boc-(*R*)-Serine	4-(Bromomethyl) benzophenone	NaH	DMF dry	Comp. 2a
MW (g/mol)	205	275.14	24		399
mMol	0.54	0.51	2.5		0.51
m	0.110 g	0.140 g	0.060 g		0.204 g
SR	1	1			
Vol.				3.5 mL	

In a double-necked flask, under nitrogen atmosphere, NaH (0.060 g; 2.5 mMol) was dissolved in DMF dry (3.5 mL). At 0°C, *N*-Boc-(*R*)-serine (0.110 g; 0.54 mMol) was added and a solution of 4-bromomethyl-benzophenone (0.140 g; 0.51 mMol) was added drop wise. The reaction was stirred at room temperature for 26 hours. The reaction was quenched with ice and HCl 2N was added arriving to pH

2 (3 mL). The water phase was extracted for three times using EtOAc (30 mL). The organic phase was washed with distillated water and brine, dried over Na_2SO_4, filtered on cotton and evaporated in vacuum. It was yellow oil (0.204 g; 0.51 mMol).

ESI-MS (Relative Abundance %): Positive: 422 (100) $[C_{22}H_{25}NO_6Na]^+$; 366 (24) $[C_{18}H_{17}NO_6Na]^+$; 322 (15) $[C_{17}H_{16}NO_4Na]^+$. Negative: 398 (100) $[M-1]^+$; 324 (55) $[C_{18}H_{14}NO_5]^+$; 211 (60)$[C_{14}H_{11}O_2]^+$.

2.4.2. (*R*)-3-(4-Benzoyl-benzyloxy)-2-*tert*-butoxycarbonylamino propionic acid cyclohexylamine salt

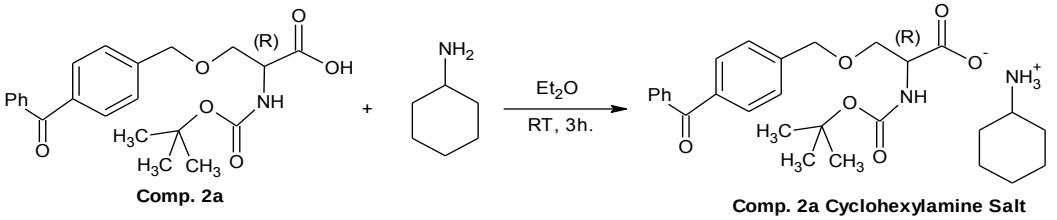

Comp. 2a **Comp. 2a Cyclohexylamine Salt**

	Comp.2a	Cyclohexyl amine	Et_2O	Comp. 2a Cyclohexylamine Salt
MW (g/mol)	399	99		498
mMol	0.51	0.51		0.41
m	0.204 g	0.050 g		0.202 g
SR	1	1		
Vol.			10 mL	

The acid (0.204 g; 0.51 mMol) was dissolved in Et_2O (10 mL) and cyclohexylamine (0.050 g; 0.51 mMol) was added on. The reaction was stirred for 3 hours at room temperature. It was filtered on gooch to have white solid (0.202 g; 0.41 mMol; yield: 80%).

ESI-MS (Relative Abundance %): Positive: 422 (100) $[C_{22}H_{25}NO_6Na]^+$; 366 (24) $[C_{18}H_{17}NO_6Na]^+$; 322 (15) $[C_{17}H_{16}NO_4Na]^+$. Negative: 398 (100) $[M-1]^+$; 324 (55) $[C_{18}H_{14}NO_5]^+$; 211 (60)$[C_{14}H_{11}O_2]^+$.

^{1}H-NMR (300 MHz $CDCl_3$, δ): 1.42 (s, 9H) $(CH_3)_3C$; 1.16-2.95(CH_2Cyclohexylamine) 3.79-3.91 (bb, 2H) OCH_2CH; 4.41 (d, 1H) OCH$_2$*CH*;

4.60 (s, 2H) PhCH_2O; 5.56 (b, 1H) CH*NH*- *t*-Boc; 7.40-7.77 (9H) aromatic protons.

Elementary Analysis: Calculated percentage: 70.13% C; 7.9% H; 6.04% N. Estimated percentage: 63.76% C; 7.24% H; 5.35% N.

[a]$_D$: -23.7

HPLC: Sample conc.: 3 mg/mL MeOH; injected vol.: 10 µL; column OD; mobile phase: Hex/*i*-PrOH/TFA; 95:5:0.05; flow: 1 mL/min.; detector: 230 nm; **E.E.: 82%**.

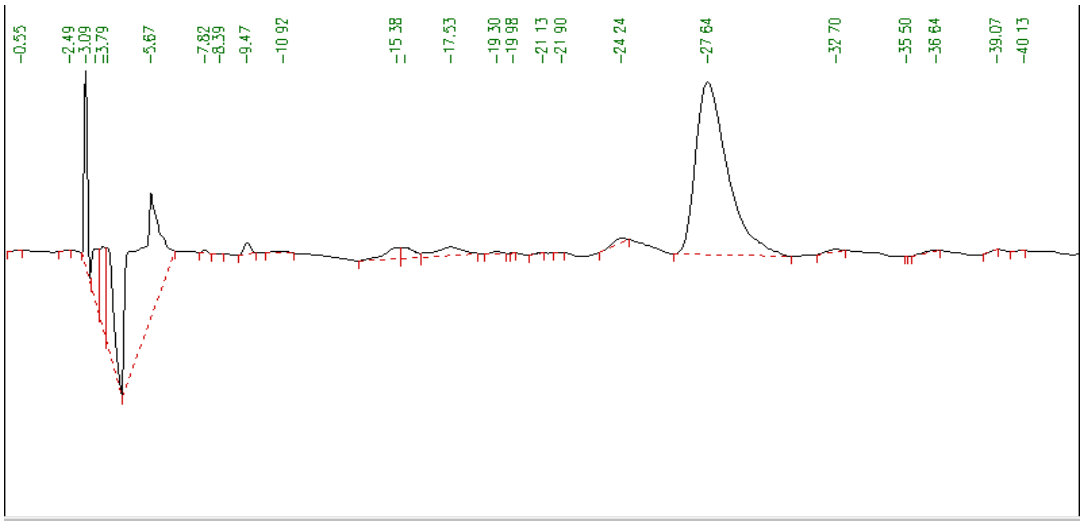

2.5. Synthetic Route of Compound 3

2.5.1. 1-Benzyl-4-(bromomethyl)benzene

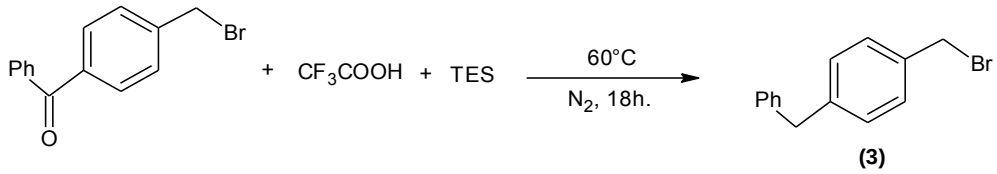

(3)

	4-(Bromomethyl) benzophenone	TFA	TES	1-Benzyl-4-(bromomethyl)-benzene (3)
MW (g/mol)	275.14	114.20	116.28	260
mMol	3.63	14.54	14.53	1.05
m	1.00 g	1.66 g	0.848 g	0.274 g
SR	1	4	4	
d (g/mL)		1.48	0.728	
Vol.		1.12 mL	1.16 mL	

In a double-necked flaks, 4-(bromomethyl)benzophenone (1.00 g; 3.63 mMol) was dissolved in TFA (1.12 mL; 14.54 mMol) under nitrogen atmosphere. TES 97% (1.16 mL; 14.53 mMol) was added and the reaction was stirred at 60°C for 18 hours. The reaction was cooled and the solution was dissolved in EtOAc. The organic layer was washed for three times with $NaHCO_3$ and once with brine. The organic layer was dried over Na_2SO_4,filtered on cotton and evaporated in vacuum to have white solid that is purified on silica gel (Hex/EtOAc 99.5:0.5- 99:1). It was white solid (0.274 g; 1.05 mMol; yield: 29%).

GC-MS (Relative Abundance %): 260 (6.1) $[C_{14}H_{13}Br]$; 181 (100) $[C_{14}H_{13}]^+$; 165 (30) $[C_{13}H_9]^+$.

^{1}H-NMR (300 MHz, $CDCl_3$, δ): 3.97 (s, 2H) $PhCH_2Ph$; 4.48 (s, 2H) $PhCH_2Br$; 7.14-7.32 (9H) aromatic protons.

2.5.2.(*R,S*)-3-(4-Benzyl-benzylsulfanyl)-2-*tert*-butoxycarbonylaminopropionic acid

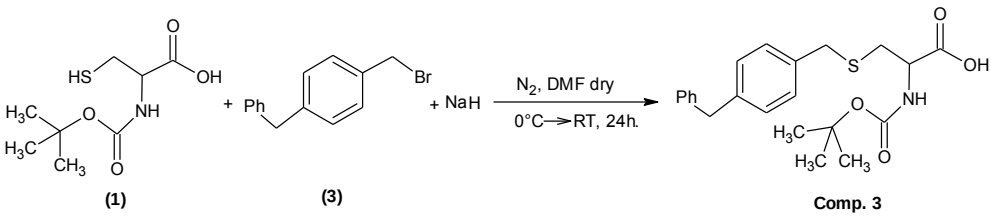

	N-Boc-(*D,L*)-Cysteine (1)	1-Benzyl-4-(bromomethyl) benzene (3)	NaH	DMF dry	Comp. 3
MW (g/mol)	221.28	260	24		401
mMol	0.91	0.82	4.17		1.23
m	0.202 g	0.214 g	0.108 g		0.492 g
SR	1	1			
Vol.				6 mL+4 mL	

In a double-necked flask, under nitrogen atmosphere, NaH (0.108 g, 4.17 mMol) was dissolved in DMF dry (6 mL). At 0°C, *N*-Boc-(*D,L*)-cysteine (0.202 g, 0.91 mMol) was added. Then, a solution of 1-benzyl-4-(bromomethyl) benzene (0.214 g, 0.82 mMol) in DMF dry (4 mL) was added drop wise. The reaction was stirred at room temperature for 24 hours. The reaction was quenched with ice and HCl 2N was added arriving to pH 2 (3 mL). The water phase was extracted for three times using EtOAc (90 mL). The organic phase was washed with distillated water and brine, dried over Na_2SO_4, filtered on cotton and evaporated in vacuum to have yellow oil (0.492 g; 1.23 mMol).

2.5.3. (*R,S*)-3-(4-Benzyl-benzylsulfanyl)-2-*tert*-butoxycarbonylamino propionic acid benzylamine salt

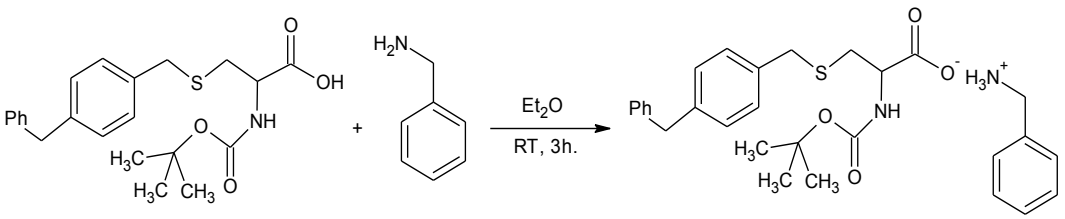

Comp. 3 **Comp. 3 Benzylamine Salt**

	Comp. 3	Benzylamine	Et_2O	Comp. 3 Benzylamine Salt
MW (g/mol)	401	107.15		508.63
mMol	1.23	1.42		0.72
m	0.492 g	0.152 g		0.367 g
SR	1	1		
Vol.			20 mL	

The acid (0.492 g; 1.23 mMol) was dissolved in Et_2O (20 mL) and on add benzylamine (0.152 g; 1.42 mMol).The reaction was stirred for 3 hours at room temperature. It was filtered to have white solid (0.367 g; 0.72 mMol; yield: 59%).

^{1}H-NMR (300 MHz $CDCl_3$, δ): 1.41 (s, 9H) $(CH_3)_3C$; 2.67-2.85 (bb, 2H) SCH_2CH; 3.62 (s, 2H) PhCH_2S; 3.91 (s, 4H) PhCH_2Ph e Ph$CH_2NH_3^+$; 4.11 (b, 1H) CH_2CHCO; 5.47 (b, 1H) CH*NH*CO; 7.06-7.33 (14H) aromatic protons.

HPLC: Sample conc.: 3 mg/1mL *i*-PrOH 10 µL; column AD; mobile phase: Hex/*i*-PrOH/TFA 80/20/0.2; flow: 1 mL/min.; l: 254 nm.

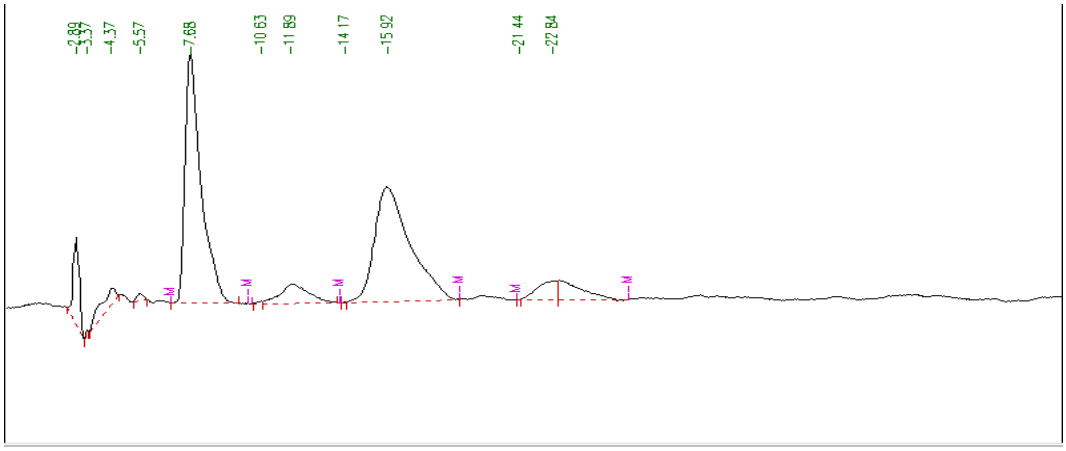

2.6. Synthetic Route of Compound 4

2.6.1. (*D,L*)-3-(4-Benzyl-benzyloxy)-2-*tert*-butoxycarbonylaminopropionic acid

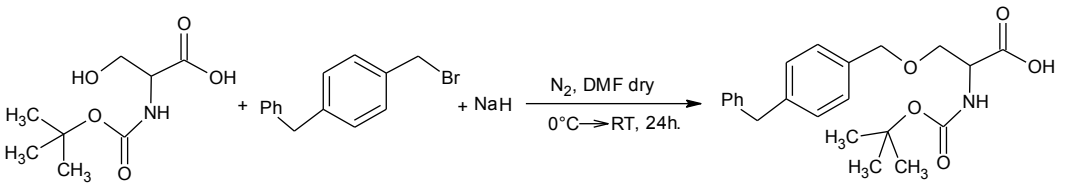

(2) (3) Comp. 4

	N-Boc-(*D, L*)-Serine (2)	1-Benzyl-4-(bromomethyl) benzene (3)	NaH	DMF dry	Comp. 4
MW (g/mol)	205	260	24		385
mMol	1.22	1.15	5.63		0.94
m	0.250 g	0.300 g	0.135 g		0.362 g
SR	1	1			
Vol.				20 mL	

In a double-necked flask, under nitrogen atmosphere, NaH (0.135 g; 5.63 mMol) was dissolved in DMF dry (20 mL). At 0°C, *N*-Boc-(*D,L*)-serine (0.250 g; 1.22 mMol) was added and a solution of1-benzyl-4-(bromomethyl)benzene (0.300 g; 1.15 mMol) was added drop wise. The reaction was stirred at room temperature for 24 hours. The reaction was quenched with ice and HCl 2N was added arriving to pH 2 (5 mL). The water phase was extracted for three times using EtOAc (60 mL). The organic phase was washed with distillated water and brine, dried over Na_2SO_4, filtered on cotton and evaporated in vacuum to have yellow oil (0.362 g; 0.94 mMol).

ESI-MS (Relative Abundance %): Positive: 408 (100) $[M+Na]^+$; 352 (24) $[C_{18}H_{18}NO_5Na]^+$; 308 (6) $[C_{17}H_{19}NO_3Na]^+$; 181 (4). Negative: 769 (17) $[2M-1]^+$; 384 (100) $[M-1]^+$; 310 (18) $[C_{16}H_{23}NO_5]$; 196 (20) $[C_{14}H_{12}O]^+$.

2.6.2. (*D,L*)-3-(4-Benzyl-benzyloxy)-2-*tert*-butoxycarbonylamino propionic acid benzylamine salt

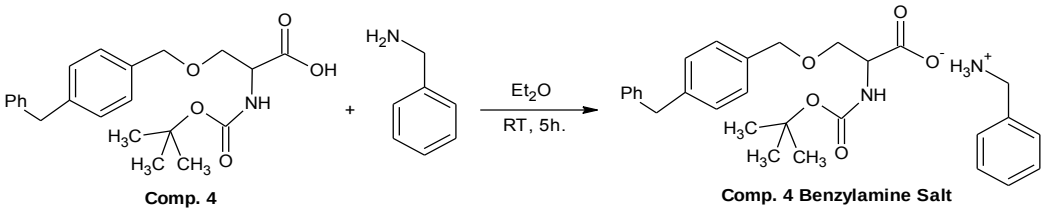

Comp. 4 Comp. 4 Benzylamine Salt

	Comp. 4	Benzylamine	Et_2O	Comp. 4 Benzylamine Salt
MW (g/mol)	385	107.15		494
mMol	0.94	0.94		0.58
m	0.362 g	0.101 g		0.286 g
SR	1	1		
Vol.			15 mL	

The acid (0.362 g; 0.90 mMol) was dissolved in Et_2O (15 mL) and benzylamine (0.101 g; 1.88 mMol) was added. The reaction was stirred for 5 hours at room temperature. It was filtered on gooch to have white solid (0.286 g; 0.58 mMol; yield: 62%).

^{1}H-NMR (300 MHz $CDCl_3$, δ): 1.39 (s, 9H) $(CH_3)_3C$; 3.60-3.69 (bb, 2H) OCH_2CH; 3.73 (s, 2H) $PhCH_2NH_3^+$; 3.89 (b, 2H) $PhCH_2Ph$; 4.01 (b, 1H) CH_2CHCOO^-; 4.34 (s, 2H) OCH_2Ph; 5.47 (d, 1H) CH*NH*- *t*-Boc; 6.46 $PhCH_2NH_3^+$; 7.06-7.36 (14H) aromatic protons.

Elementary Analysis: Calculated percentages: 70.70% C; 7.38% H; 5.68% N. Estimated percentages: 70.24% C; 7.27% H; 5.70% N.

HPLC: Sample conc.: 3 mg/mL *i*-PrOH 10 µL; column AD; mobile phase: Hex/*i*-PrOH/TFA 80:20:0.1; flow: 1 mL/min.; detector: 230 nm.

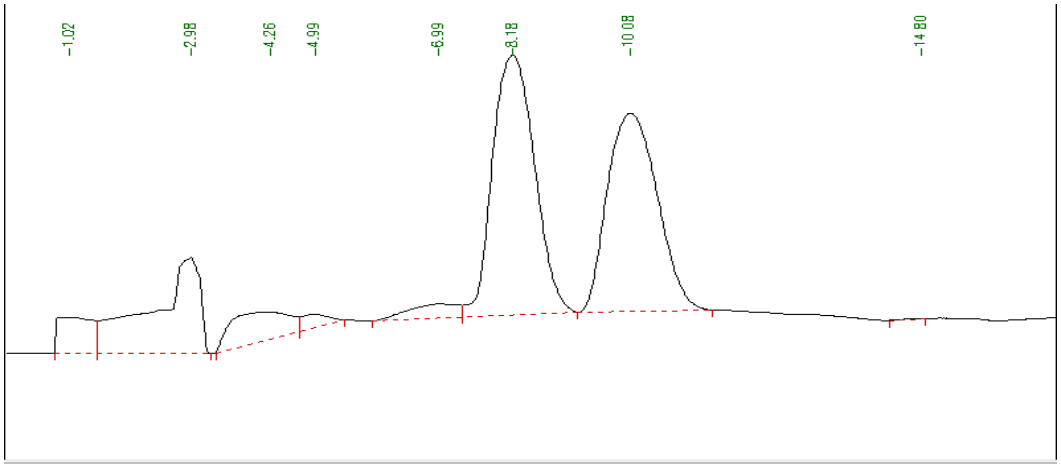

2.7. Synthesis Route of Compound 5 and 5a

2.7.1. (*R*)-3-(Biphenyl-4-ylmethylsulfanyl)-2-*tert*-butoxycarbonylamine propionic acid methyl ester

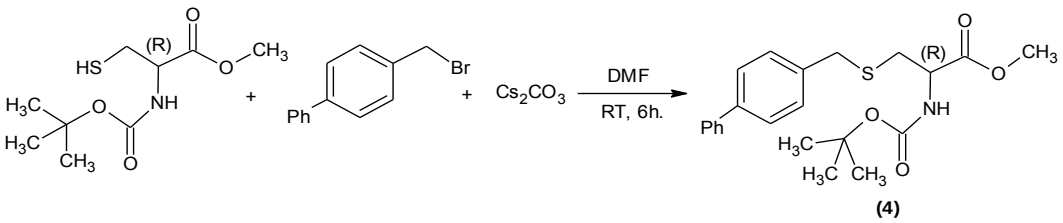

(4)

	N-Boc-(*L*)-Cysteine Methyl Ester	4-(Bromomethyl) biphenyl	Cs_2CO_3	DMF	(4)
MW (g/mol)	235.30	247	325.82		401.30
mMol	1.88	2.02	4.04		1.62
m	0.443 g	0.500 g	1.317 g		0.650 g
SR	1	1			
Vol.				20 mL	

4-(Bromomethyl)biphenyl (0.500 g; 1.88 mMol) was dissolved in DMF (20 mL); Cs_2CO_3 (1.317 g; 4.04 mMol) and *N*-Boc-(*L*)-cysteine methyl ester (0.443 g; 2.02 mMol) were added to the solution. The reaction was stirred at room temperature for 6 hours, and then it was quenched adding 20 mL of distillated water. The water layer was extracted three times using EtOAc. The organic layer was washed with brine, dried over Na_2SO_4, filtered on cotton and evaporated in vacuum, having a yellow oil, that is purified on silica gel (Hex/EtOAc 8:2). It was transparent oil (0.650 g; 1.62 mMol; yield: 86%).

ESI-MS (Relative Abundance %): Positive: 424(100) $[C_{22}H_{27}NSO_4Na]^+$; 368 (13) $[C_{18}H_{18}NSO_4Na]^+$; 324 (4), $[C_{17}H_{18}NSO_2Na]^+$;

^{1}H-NMR (300 MHz, $CDCl_3$, δ): 1.46 (s, 9H) CH_3C; 2.81-2.92 (bb, 2H) SCH_2CH; 3.75 (s, 3H) CH_3CO; 3.76 (s, 2H) $PhCH_2S$; 4.56 (b, 1H) CH_2CHCO; 5.32 (b, 1H) CHNHCO; 7.31-7.60 (9H) aromatic protons.

2.7.2. (*R,S*) and (*R*)-3-(Biphenyl-4-ylmethylsulfanyl)-2-*tert*-butoxycarbonylamino propionic acid

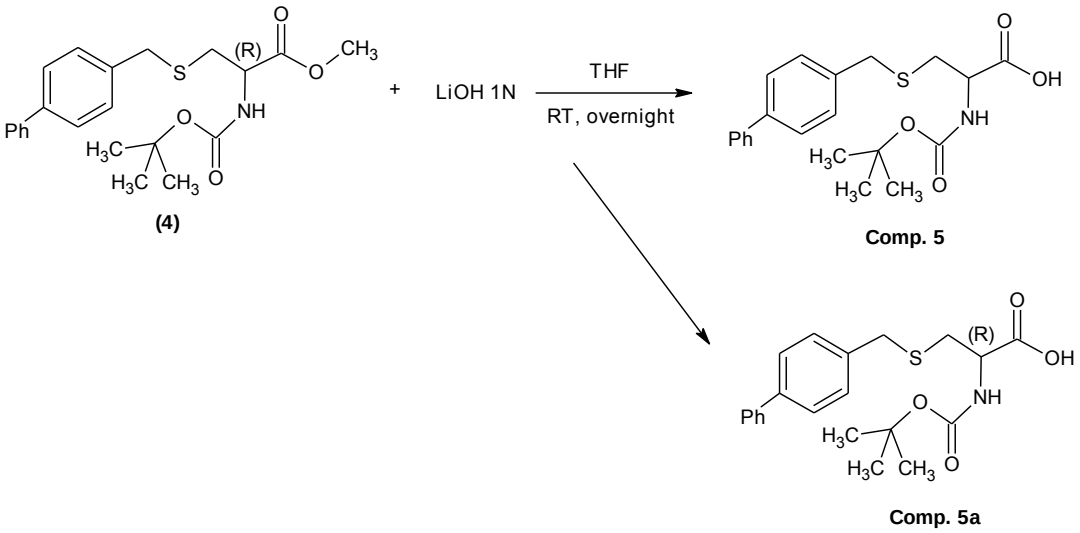

	(4)	LiOH 1N	THF	Comp. 5 and 5a
MW (g/mol)	401.30			387
mMol	1.62			1.51
m	0.650 g			0.585 g
SR	1	1		
Vol.		10 mL	10 mL	

3-(Biphenyl-4-ylmethylsulfanyl)-2-*tert*-butoxycarbonylamino propionic acid methyl ester (0.650 g; 1.62 mMol) was dissolved in THF (10 mL) and LiOH 1N (10 mL) was added. The reaction was stirred at room temperature overnight. Then HCl 2N (4.5 mL) was added and the water layer was extracted three times with Et_2O. The organic layer was washed with brine, dried over Na_2SO_4 filtered on cotton and evaporated in vacuum to have white semi-solid (Crude: 0.585 g; 1.51 mMol).

ESI-MS (Relative Abundance %): Positive: 410 (100) $[C_{21}H_{25}NSO_4Na]^+$; 354 (10) $[C_{17}H_{16}NSO_4Na]^+$; 310 (4) $[C_{16}H_{16}NSO_4Na]$. Negative: 773 (14) [2M-1]; 386 (100) $[C_{21}H_{24}NSO_4]^+$; 312 (37) $[C_{17}H_{13}NSO_3]^+$; 199 (50)$[C_{13}H_{11}S]^+$.

^{1}H-NMR (300 MHz $CDCl_3$, δ): 2.90-2.94 (bb, 2H) SCH_2CH; 3.75 (s, 3H) CH_3CO; 3.79 (s, 2H) $PhCH_2S$; 4.50 (s, 1H) CH_2CHCO; 5.32 (b, 1H) CHNHCO; 7.31-7.63 (9H) aromatic protons.

Crude: 0.585 g

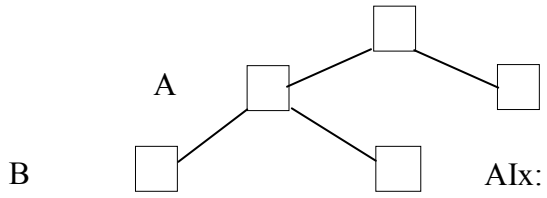

Ix: 0.135 g (**Comp. 5**)
(0.35 mMol; yield 22%)

AIx: 0.130 g (**Comp. 5a**)
(0.34 mMol; yield %21)

Elementary Analysis AIx: Calculated percentages: 65.09% C; 6.50% H; 3.61%N. Estimated percentages: 63.81% C; 6.57% H; 3.62% N.

Melting Point Ix: 132.8-134.2 °C.

Melting Point AIx: 78.6-79.8 °C.

$[a]_D$ Ix:-0.5

$[a]_D$ AIx:-29

HPLC Ix: Sample conc.:3 mg/mL *i*-PrOH 10 µL; column OD; mobile phase: Hex/*i*-PrOH/TFA 90:10:0.25; flow: 1 mL/min; detector: 230 nm.

HPLC AIx: Sample conc.: 2 mg/mL *i*-PrOH 5 µL; column OD; mobile phase: Hex/*i*-PrOH/TFA 90:10:0.25; flow: 1 mL/min; detector: 230 nm; **E.E.: 91%**.

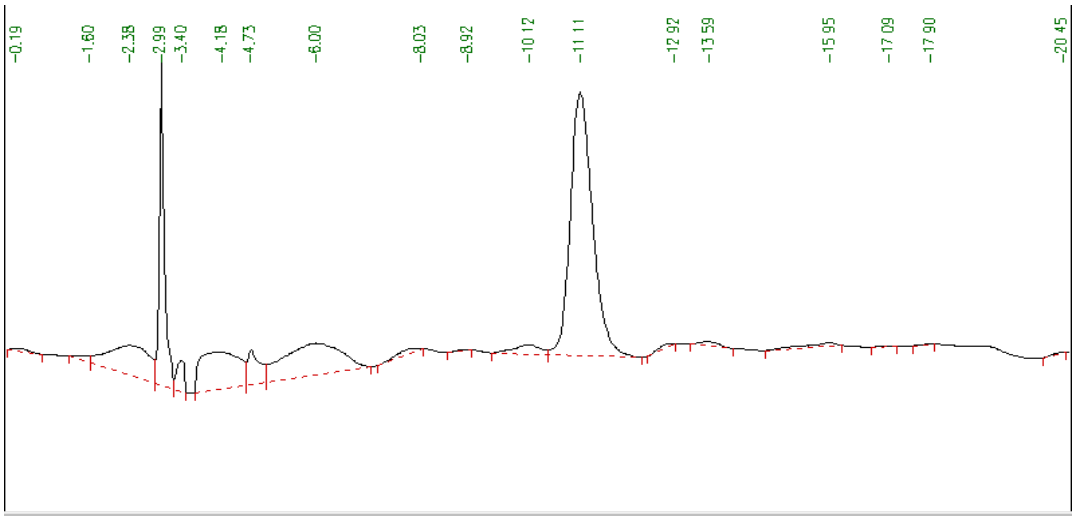

HPLC Ix: Sample conc.: 3 mg/mL *i*-PrOH 10 µL; column OD; mobile phase: Hex/*i*-PrOH/TFA 95:5:0.05; flow: 1 mL/min; detector: 230 nm

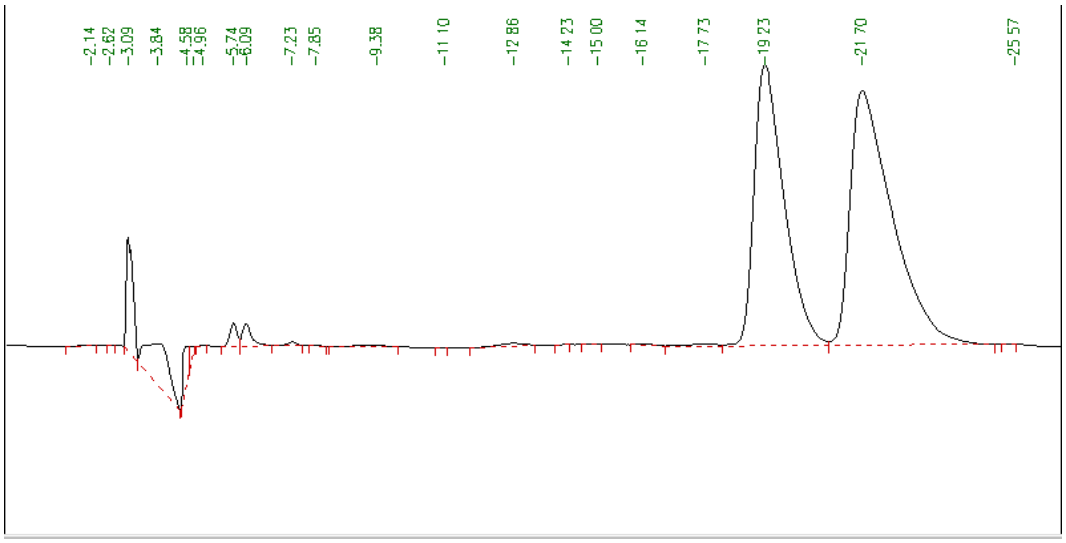

HPLC Mother Liquor B: Sample conc.: 2 mg/mL *i*-PrOH 10 µL; column OD; mobile phase: Hex/*i*-PrOH/TFA 95:5:0.05; flow: 1 mL/min; detector: 230 nm; **E.E.: 99%**.

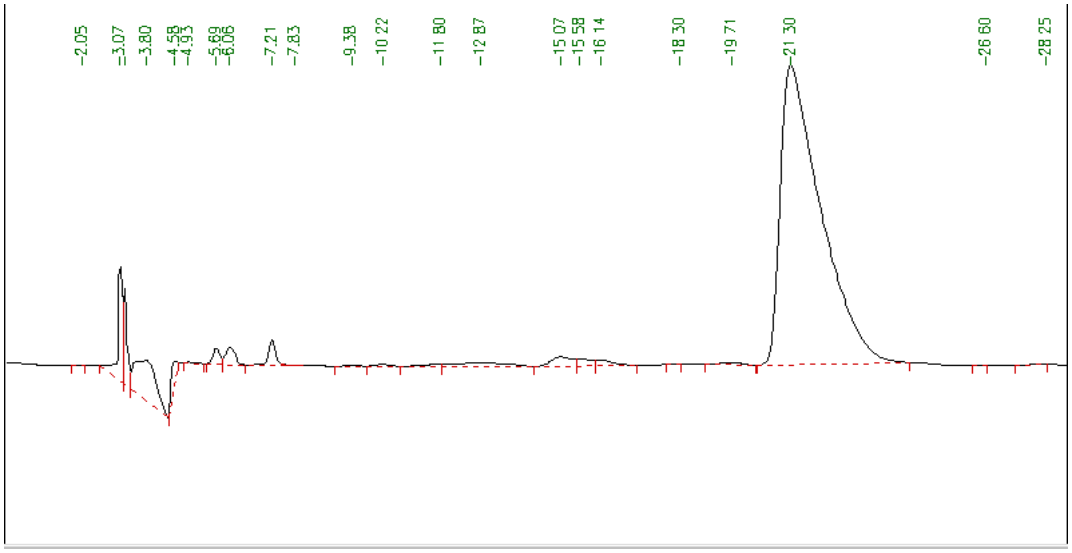

2.8. Synthesis Route of Compound 6

2.8.1. 3-(Biphenyl-4-ylmethoxy)-2-*tert*-butoxycarbonylamino-propionic acid

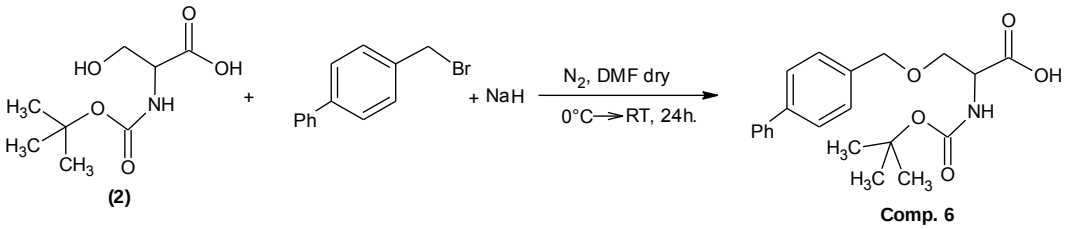

	N-Boc-(*D,L*)-Serine	4-(Bromomethyl) biphenyl	NaH	DMF dry	Comp. 6
MW (g/mol)	205.21	247	24		371
mMol	2.05	2.02	8.88		1.71
m	0.421 g	0.500 g	0.213 g		0.635 g
SR	1	1			
Vol.				15 mL +5 mL	

In a double-necked flask, under nitrogen atmosphere, NaH (0.213 g; 8.87 mMol) was dissolved in DMF dry (15 mL). At 0°C, *N*-Boc-(*D,L*)-serine (0.421 g; 2.05 mMol) was added and a solution of 4-bromomethyl-dipehnyl (0.500 g; 2.02 mMol) in DMF dry (5 mL) was added drop wise. The reaction was stirred at room temperature for 24 hours. The reaction was quenched with ice and HCl 2N was added arriving to pH 2 (5 mL). The water phase was extracted for three times using EtOAc (60 mL). The organic phase was washed with distillated water and brine, dried over Na_2SO_4, filtered on cotton and evaporated in vacuum. It was yellow oil (0.635 g; 1.71 mMol).

ESI-MS (Relative Abundance %): Positive: 394 (100) $[M+Na]^+$; 338 (44) $[C_{17}H_{16}NO_5Na]^+$; 294 (12) $[C_{16}H_{16}NO_3Na]^+$. Negative: 370 (100) $[M-1]^+$; 296 (18) $[C_{17}H_{13}NO_4]^+$; 183 (10) $[C_{13}H_{11}O]^+$.

2.8.2. 3-(Biphenyl-4-ylmethoxy)-2-*tert*-butoxycarbonylamino-propionic acid benzylamine salt

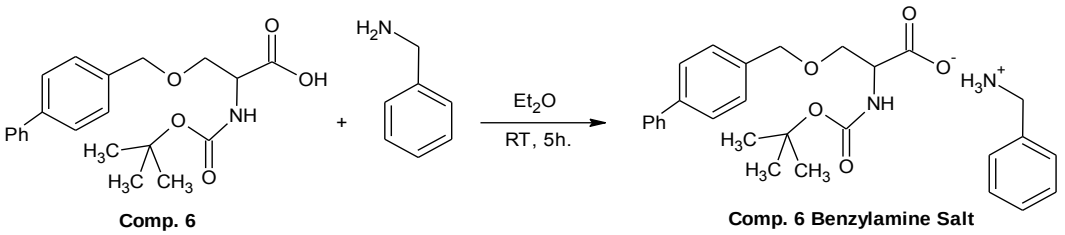

Comp. 6 **Comp. 6 Benzylamine Salt**

	Comp. 6	Benzylamine	Et_2O	Comp. 6 Benzylamine Salt
MW (g/mol)	371	107.15		478.15
mMol	1.71	1.74		0.60
m	0.635 g	0.186 g		0.286 g
SR	1	1		
Vol.			30 mL	

The acid (0.635 g; 1.71 mMol) was dissolved in Et_2O (30 mL) and cyclohexylamine (0.186 g; 1.74 mMol) was added on. The reaction was stirred for 5 hours at room temperature. It was filtered on gooch to have white solid (0.286 g; 0.60 mMol; yield: 35%).

^{1}H-NMR (300 MHz $CDCl_3$, δ): 1.40 (s, 9H) $(CH_3)_3C$; 3.62-3.76 (bb, 2H) OCH_2CH; 3.85 (s, 2H) $PhCH_2NH_3^+$; 3.92-4.08 (b, 1H) CH_2CHCOO^- ; 5.52 $PhCH_2NH_3^+$; 5.84(b, 1H) CH*NH*- *t*-Boc; 7.26-7.52 (14H) aromatic protons.

Elementary Analysis: Calculated percentage: 70.44% C; 7.13% H; 5.82% N. Estimated percentage: 61.96% C; 6.95% H; 6.66% N.

HPLC: Sample conc.2 mg/mL MeOH; injected vol.5 µL; column OD; mobile phase: Hex/*i*-PrOH/TFA 90:10:0.25; flow 1 mL/min; detector: 230 nm.

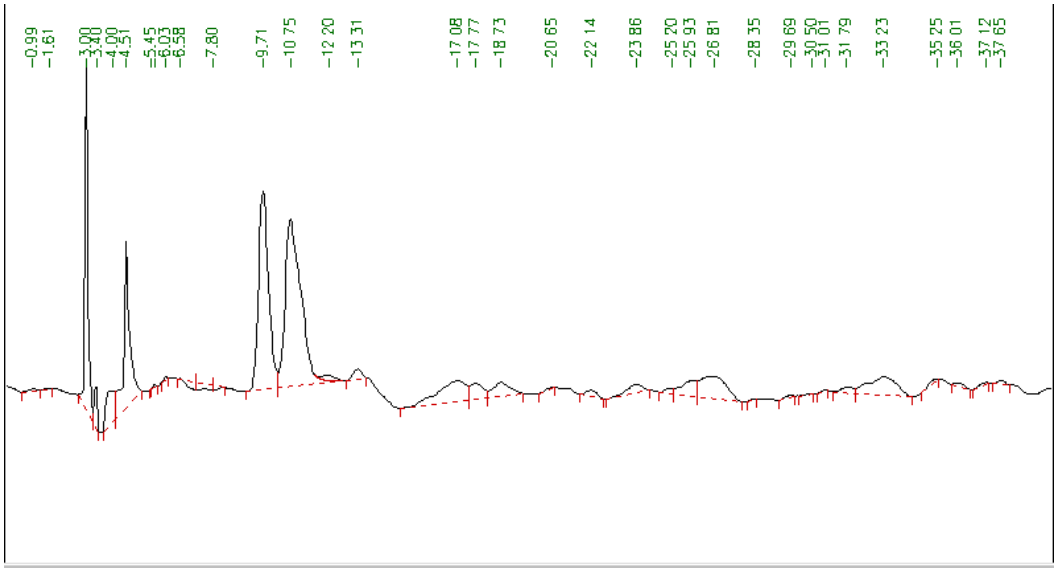

BIOLOGICAL ASSAYS

To evaluate biological activity on PPARs, tests were made on transfection assay using HepG2 cell line, for GAL4-PPAR transactivation.

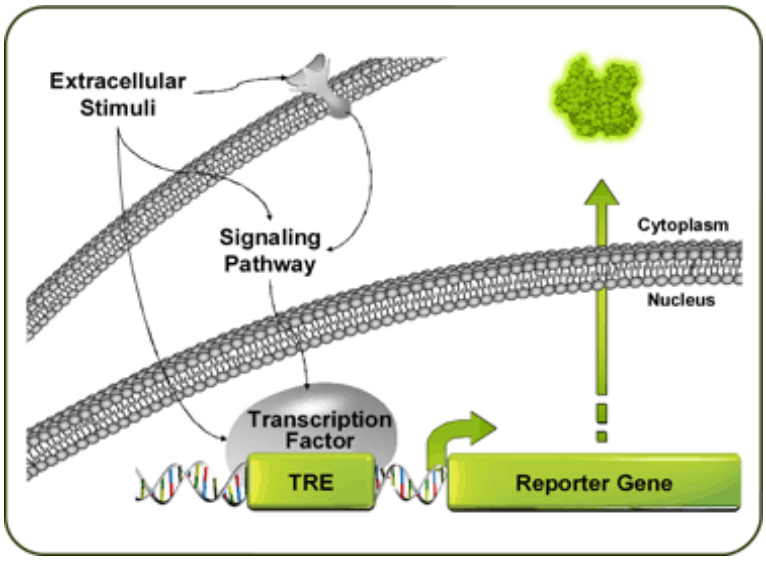

Figure 18. PPAR Transfection assay.

On this way was used chimeric codified by a plasmid, called pGAL4 PPARα or γ, where PPAR-LDB is linked to the transcriptional factor GAL4 DBD. This plasmid is transfected with a reporter gene that codifies to luciferase

(pGal5TKpGL3), drown by different response elements (Gal4 response element) and by Herpes simplex virus thymidine-kinase promoter. Because of mammalian cells don't have GAL4, only chimeric receptor GAL4-PPAR is able to active gene reporter.

Variation of luciferase levels will give information about different activation of PPAR by compound tested. The activity of WY14,643 and Rosiglitazone, used like references for PPARα and PPARγ respectively, were 100.

Compound we were tested using this experimental approach and data were reported on the Table 3.

	PPARα		PPARγ		PPARβ/δ	
Molecule	EC_{50} (μM)	Efficacy (%)	EC_{50} (μM)	Efficacy (%)	EC_{50} (μM)	Efficacy (%)
Wy14,643	1.6	100	-	-	-	-
Rosiglitazone	-	.	0.039	100	-	-
Comp.1	**1.6**	**83**	**10.3**	**15**	**37**	**71**
Comp. 2	11	46	20	15	-	5
Comp. 3	0.7	65	3	21	-	10
Comp. 4	10	52	-	7	-	2
Comp. 5	0.9	106	3	29	-	8
Comp.6	7.2	100	13	20	-	0

Table 3. Biological activity values on PPARs of compounds.

From these data it is clear that all synthesized molecules have good business competitiveness respectively on full or partial PPARα and PPARγ, but compared to AL26-18 (**Comp. 1**), lose activity on the PPARδ/β. In some cases, the activity on PPARα proves to be even better compared to the compounds used as reference, AL26-18. In addition, the structural modifications to the load benzophenonic portion are able to reduce the activity of the molecule on the receptor PPARα, as in the case of **Comp. 3** and **4.** Sulfur substituted **Comp. 1**, **3** and **5** have better

activation than oxygen substituted **Comp. 2**, **4** and **6** on the PPARα and PPARγ, both. By biological tests carried out inside of our research team, therefore, it was found that the resulting molecule more active was AL26-18, so it was decided to continue the series of structural modifications at the expense of this compound.

CONCLUSION

In the present study, was focused on to Niemann-Pick Type C disease, not type A, B or D, because Niemann-Pick Type A and B are the result of accumulation of sphingomyelin and these diseases generally are characterized deficiency of sphingomyelinase. When NPC compare with Niemann-Pick Type D it is more common disease than type D.

Compound 1, **1a**, **2**, **2a**, **3**, **4**, **5**, **5a** and **6** were synthesized led by derived clofibrate AL26-18 to creating new scaffold as PPAR agonists for further investigation as potential therapeutics for NPC disease. These compounds were derived based on SAR information of some compounds, derived from clofibrate, in the previous studies (Fig 13). Among them, **Comp. 1a**, **2a** and **5a** are isoster molecules. Their $[\alpha]_D$ values and E.E. are +2, 97%; -23.7, 82% and -29, 91%, respectively.

Comp. 1, **2**, **2a**, **3**, **4** and **6** were synthesized as in Fig 16. Synthesized in optically active form compounds, **Comp. 1a** and **5a** have a different synthetic route from others (Fig 17). During the synthesis **Comp. 5a**, also was obtained **Comp. 5**. All Compounds were oil except **Comp. 5** and **5a**. While all of these compounds' analysis results were operating on their cylohexylamine or benzylamine salts which were obtained by acid-base (salt) reactions, **Comp. 5**and **5a** could been crystalized that used for their analyses.

Yield % of compounds weren't so high. The highest yield was %80 for **Comp. 2a** and the lowest yield was %21 for **Comp. 5a** (Table 4).

^{1}H-NMR data for compounds are presented in experimental section for each compound. All *t*-Boc protons were observed at 1.39-1.42 ppm as singlet and all

aromatic protons were signal at expected 7.07-7.77 ppm by depending on shielding effect. While aliphatic methyl protons of sulfur substituted **Comp. 1**, **1a**, **3** and **5** (Ph*CH*$_2$S) were seen at 3.62-3.79 ppm as singlet, aliphatic methyl protons of oxygen substituted **Comp. 2**, **2a**, **4** and **6** (Ph*CH*$_2$O) were seen at4.34-5.52 ppm as singlet. Methyl protons belong to cyclohexylamine of **Comp. 2** and **2a**(CH_2Cyclohexylamine) and to benzylamine of **Comp. 1**, **1a**, **3**, **4** and **6** ($PhCH_2NH_3^+$) are at 1.16-2.95 and 3.73-3.98, respectively (Table 4).

Biological activity results show that all compounds that are full agonist for PPARα and partial agonists for PPARγare dual agonist, and have good values compared to the compounds used as reference, but they lose activities on the PPARδ/β. Even, activity on PPARα of **Comp. 5** and **Comp. 6** are better than AL26-18. Also, the most effective compounds on PPARγ are **Comp. 5** and **6.** The structural modifications of lead compound on benzophenonic portion are able to reduce the activity of the molecule on the receptor PPARα, as in the case of **Comp. 3** and **4.**

In the light of this study, some of the synthesized pan-agonist compounds could be as a new potential therapeutic leads for NPC disease for further investigation via down-regulating of NPC1L1 gene expression.

Code	Compound	^{1}H-NMR (300 MHz $CDCl_3$, δ)	Yield (%)
Comp. 1 Salt	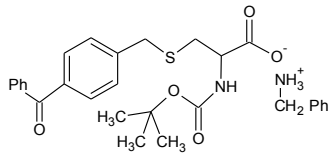	1.41 (s, 9H) (CH_3)$_3$C; 2.72-2.95 (bb, 2H) SCH_2CH; 3.72 (s, 2H) PhCH_2S; 3.95 (s, 2H) Ph$CH_2NH_3^+$; 4.15 (b, 1H) CH_2CHCOO$^-$; 5.54 (b, 1H) CH*NH*- *t*-Boc; 7.28-7.76 (14H) aromatic protons.	39
Comp. 1a Salt	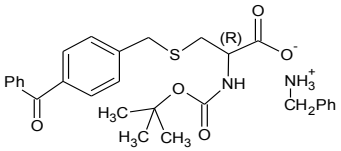	1.42 (s, 9H) (CH_3)$_3$C; 2.74-2.88 (bb, 2H) SCH_2CH; 3.73 (s, 2H) PhCH_2S; 3.98 (s, 2H) Ph$CH_2NH_3^+$; 4.19 (b, 1H) CH_2CHCOO$^-$; 5.44 (b, 1H) CH*NH*- *t*-Boc; 7.30-7.77 (14H) aromatic protons.	61
Comp. 2 Salt	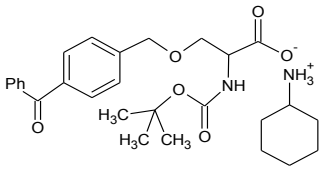	1.42 (s, 9H) (CH_3)$_3$C; 1.16-2.95(CH_2Cyclohexylamine) 3.79-3.91 (dd, 2H) OCH_2CH; 4.41 (d, 1H) OCH_2CH; 4.60 (s, 2H) PhCH_2O; 5.56 (d, 1H) CH*NH*- *t*-Boc; 7.40-7.77 (9H) aromatic protons.	40
Comp. 2a Salt	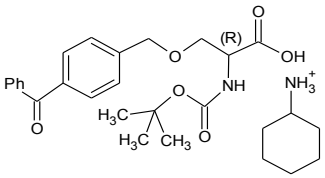	1.42 (s, 9H) (CH_3)$_3$C; 1.16-2.95(CH_2Cyclohexylamine) 3.79-3.91 (bb, 2H) OCH_2CH; 4.41 (d, 1H) OCH_2CH; 4.60 (s, 2H) PhCH_2O; 5.56 (b, 1H) CH*NH*- *t*-Boc; 7.40-7.77 (9H) aromatic protons.	80
Comp. 3 Salt	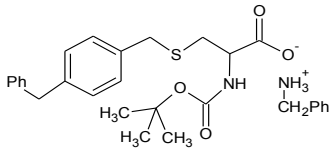	1.41 (s, 9H) (CH_3)$_3$C; 2.67-2.85 (bb, 2H) SCH_2CH; 3.62 (s, 2H) PhCH_2S; 3.91 (s, 4H) PhCH_2Ph and Ph$CH_2NH_3^+$; 4.11 (b, 1H) CH_2CHCO; 5.47 (b, 1H) CH*NH*CO; 7.06-7.33 (14H) aromatic protons.	59
Comp. 4 Salt	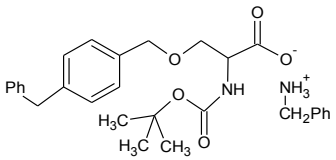	1.39 (s, 9H) (CH_3)$_3$C; 3.60-3.69 (bb, 2H) OCH_2CH; 3.73 (s, 2H) Ph$CH_2NH_3^+$; 3.89 (b, 2H) PhCH_2Ph; 4.01 (b, 1H) CH_2CHCOO$^-$; 4.34 (s, 2H) PhCH_2O; 5.47 (d, 1H) CH*NH*- *t*-Boc; 6.46 Ph$CH_2NH_3^+$; 7.06-7.36 (14H) aromatic protons.	62
Comp. 5	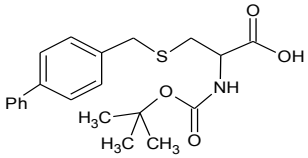	2.90-2.94 (bb, 2H) SCH_2CH; 3.75 (s, 3H) CH_3CO; 3.79 (s, 2H) PhCH_2S; 4.50 (s, 1H) CH_2CHCO; 5.32 (b, 1H) CH*NH*CO; 7.31-7.63 (9H) aromatic protons.	22
Comp. 5a	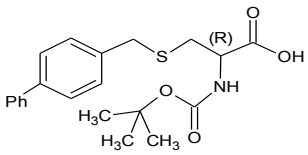	No data.	21
Comp. 6 Salt	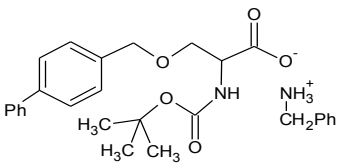	1.40 (s, 9H) (CH_3)$_3$C; 3.62-3.76 (bb, 2H) OCH_2CH; 3.85 (s, 2H) Ph$CH_2NH_3^+$; 3.92-4.08 (b, 1H) CH_2CHCOO$^-$; 5.52 (s, 2H) PhCH_2O; 5.84(b, 1H) CH*NH*- *t*-Boc; 7.26-7.52 (14H) aromatic protons.	35

Table 4. Listof ^{1}H-NMR and yield valuesof compounds.

REFERENCES

Altınışık M., ‘‘Lipidlerin Yapısal ve İşlevsel Özellikleri VII,’’ (http://www.belgeler.com/blg/1l1s/lipidlerin-yapisal-ve-islevsel-ozellikleri-vii), ADÜFT Biyokimya AD, 2006

Buckle D.R., Cantello B.C.C., Cawthorne M.A., Coyle P.J., Dean D.K., Faller A., Haigh D., Hindley R.M., Jefcott L.J., Lister C.A., Pinto I.L., Rami H.K., Smith D.G., Smith S.A., “Non thiazolidinedione anti hyperglycaemic agents .1. alpha-heteroatom substituted beta-phenylpropanoic acids”, *Bioorg. Med. Chem. Lett.,* **6(17)**, 2121-2126, 1996.

Carrieri A, Giudici M, Parente M, De Rosas M, Piemontese L, Fracchiolla G, Laghezza A, Tortorella P, Carbonara G, Lavecchia A, Gilardi F, Crestani M, Loiodice F., “Molecular determinants for nuclear receptors selectivity: chemometric analysis, dockings and site-directed mutagenesis of dual peroxisome proliferator-activated receptors α/γ agonists”, *Eur. J. Med. Chem.,* 63, 321-332, 2013.

Cobb, J.E., Blanchard S.G., Boswell E.G., Brown K.K., Charifson P.S., Cooper J.P., Collins J.L., Dezube M., Henke B.R., Hull-Ryde E.A., Lake D.H., Lenhard J.M., Oliver W., Oplinger Jr. J., Pentti M., Parks D.J., Plunket K.D., and Tong W.-Q., “*N*-(2-Benzoylphenyl)-L-tyrosine PPARγ Agonists. 3. Structure−Activity Relationship and Optimization of the *N*-Aryl Substituent,” *J. Med. Chem.,* **41**, 5055-5069, 1998.

Coll T., Rodríguez-Calvo R., Barroso E., Serrano l., Eyre E., Palomer X. and Vázquez-Carrera M., ‘‘Peroxisome Proliferator-Activated Receptor (PPAR)β/δ: A New Potential Therapeutic Target for the Treatment of Metabolic Syndrome,’’ *Current Molecular Pharmacology*, **2**, 46-55, 2009

Collins, J.L., Blanchard S.G., Boswell G.E., Charifson P.S., Cobb J.E., Henke B.R., Hull-Ryde E.A., Kazmierski W.M., Lake D.H., Leesnitzer L.M., Lehmann J., Lenhard J.M., Orband-Miller L.A., Gray-Nunez Y., Parks D.J., Plunkett K.D., and Tong W.-Q., “*N*-(2-Benzoylphenyl)-L-tyrosine PPARγ Agonists. 2.

Structure−Activity Relationship and Optimization of the Phenyl Alkyl Ether Moiety", *J. Med. Chem.,* **41**, 5037-5054, 1998.

Fantini J., Garmy N., Mahfoud R., Yahi N., "Lipid rafts: structure, function and role in HIV, Alzheimer's and prion diseases", Structure-based classification of membrane lipids, ExpertsReviews in MolecularMedicine, 1, 2002.

Fiedorek F.T., Wilson G.G., Frith L., Patel J., Abou-Donia M.,StudyGroup, PPA20005. "Mono therapy with GI262570, a tyrosine-basednon-thiazolidinedione PPAR-gamma agonist, improves metabolic control in type 2 diabetesmellituspatients". Program and Abstracts of the 60th Scientific Sessions of the American Diabetes Association; June 9-13, 2000; San Antonio, Texas. Abstract 157-OR. *Diabetes*, **49**, 38, 2000.

Floyd C.D., "Metalloproteinase Inhibitors", *WO9823588 (A1),*4 June 1998.

Gampe R.T., Montana V.G., Lambert M.H., Miller A.B., Bledsoe R.K., Milburn M.V., Kliewer S.A., Willson T.M., Xu H.E., "Asymmetry in the PPAR gamma/RXR alpha crystal structure reveals the molecular basis of heterodimerization among nuclear receptors*", Mol. Cell,* **5(3)**, 545-555, 2000.

Gazioğlu S.B., *Lipit Depo Hastalıkları,* Yüksek Lisans Projesi, Yakın Doğu Üniversitesi, Sağlık Bilimleri Enstitüsü, Lefkoşa, 2012.

Gelmez Beker D. and Aliyazıcıoğlu Y., ''Lizozomal Depo Hastalıklarının Tanı ve Tedavisinde Yeni Yaklaşımlar,'' *O.M.Ü. Tıp Dergisi /J. Exp. Clin. Med.*, 19[1], 78-82, 2002.

Golinski M, Delaluz P.J., Delcamp T.J., Watt D.S., Vanaman T.C., "Synthesis and Binding-Affinity of bidentate Phenothiazines with 2 different photoactive groups", Bioconjugate Chemistry, **6(5)**, 567-572, 1995.

Gottumukkala V.S., Hindupur R.M., "Novel StilbeneAnalogs", *WO2010046926 (A2),* 29 Apr 2010.

Henke B.R., Blanchard S.G., Brackeen M.F., Brown K.K., Cobb J.E., Collins J.L., Harrington W.W., Hashim Jr. M.A., Hull-Ryde E.A., Kaldor I., Kliewer S.A.,

Lake D.H., Leesnitzer L.M., Lehmann J.M., Lenhard J.M., Orband-Miller L.A., Miller J.F., Mook R.A., Noble Jr.S.A., Oliver W., Parks Jr. D.J., Plunket K.D., Szewczyk J.R., and Willson T.M., "*N*-(2-Benzoylphenyl)-L-tyrosine PPARγAgonists. 1. Discovery of a Novel Series of Potent Antihyperglycemic and Antihyperlipidemic Agents", *J. Med. Chem.,* **41**, 5020-5036, 1998.

Howell K.L., DeVita R.J., Garcia-Calvo M., Meurer M.D., Lisnock J., Bull H. G., McMasters D.R., McCann M.E. and Mills S.G., *Bioorg. Med. Chem. Lett.,***20**, 6929-6932, 2010.

Hulin B., McCarthy P.A., Gibbs E.M., "The glitazone family of antidiabetic agents", *Curr. Pharm. Design,* **2(1)**, 85-102, 1996.

Iwayanagi Y., Takada T., Tomura F., Yamanashi Y., Terada T., Inui K. and Suzuki H., ''Human NPC1L1 Expression is Positively Regulated by PPARα,'' *Pharm. Res.,* **28**, 405-412, 2011.

Jackson T.A., Richer J.K., Bain D.L., Takimoto G.S., Tung L., Horwitz K.B., "The partial agonist activity of antagonist-occupied steroid receptors is controlled by a novel hinge domain-binding co-activator L7/SPA and the co-repressors N-CoR or SMRT", *Mol. Endocrinol.,* **11(6)**, 693-705, 1997.

Kersten S. and Wahli W., *New Approaches to Drug Development*, P. Jolles, Ed. BirkhauserVerlag, Switzerland, 2000.

Lawrence R.A., "Phosphinate based inhibitors of matrix metalloproteases", US6147061 (A), 14 November 2000.

Lee M.R., Jung D.W., Williams D. and Shin I.J., "Efficient solid-phase synthesis of trifunctional probes and their application to the detection of carbohydrate-binding proteins," *Org. Lett.*, 7(24), 5477-5480, 2005.

McMasters D. R., Garcia-Calvo M., Maiorov V., McCann M. E., Meurer M. D., Bull H. G., Lisnock J., Howell K.L. and DeVita R.J., ''Spiroimidazolidinone NPC1L1 inhibitors. 1: Discovery by 3D-similarity-based virtual screening,'' *Bioorg. Med. Chem. Lett.,***19**, 2965-2968, 2009.

Mukherjee R., Jow L., Croston G.E., Paterniti J.R., "Identification characterization, and tissue distribution of human peroxisome proliferator-activated receptor (PPAR) isoforms PPAR gamma 2 versus PPAR gamma 1 and activation with retinoid X receptor agonists and antagonists", *J. Biol. Chem.,* **272(12)**, 8071-8076, 1997.

Nagy L., Tontonoz P., Alvarez J.G.A., Chen H.W., Evans R.M., "Oxidized LDL regulates macrophage gene expression through ligand activation of PPAR gamma", *Cell,* **93(2)**, 229-240, 1998.

Nelson, D.L.,Cox, M.M., LehningerPrinciples of Biochemistry, W.H. FreemanandCompany, New York, 1119s, 2005.

Nolte R.T., Wisely G.B., Westin S., Cobb J.E., Lambert M.H., Kurokawa R., Rosenfeld M.G., Willson T.M., Glass C.K., Milburn M.V., "Ligand binding and co-activator assembly of the peroxisome proliferator-activated receptor-gamma", *Nature,* **395**, 137-143, 1998.

Pacheco C.D., *Autophagy and tau in Niemann-Pick type C disease*, The University of Michigan, 2008.

Pfefferkorn J.A., Larsen S.D., Huis C.V., Sorenson R., Barton T., Winters T., Auerbach B., Wu C., Wolfram T.J., Cai H., Welch K., Esmaiel N., Davis J., Bousley R., Olsen K., Mauller S. B. and Mertz T., ''Substituted oxazolidinones as novel NPC1L1 ligands for the inhibition of cholesterol absorption,'' *Bioorg. Med. Chem. Lett.,***18**, 546–553, 2008.

Rosenbaum A.I., Cosner C.C., Mariani C.J., Maxfield F.R., Wiest O. and Helquist P., ''ThiadiazoleCarbamates: Potent Inhibitors of Lysosomal Acid Lipase and Potential Niemann-Pick Type C Disease Therapeutics,'' *J. Med. Chem.,* **53**, 5281–5289, 2010.

Schow S.R., Aurrecoechea N., "Tripeptide and tetrapeptidesulfones," *US7192918 (B2),* 20 March 2007.

Shearer B.G., Hoekstra W.J., ‘‘Peroxisome Proliferator-Activated Receptors (PPARs): Choreographers of Metabolic Gene Transcription,’’ *Celltransmissions*, **18**, No.3, 1-10, 2003.

Spiegelman B.M. and Flier J.S., “Adipogenesis and obesity: Rounding out the big picture”, *Curr. Opin. Cell Biol.,* **87(3)**, 377-389, 1996.

Uppenberg J., Svensson C., Jaki M., Bertilsson G., Jendeberg L., Berkenstam A., “Crystal structure of the ligand binding domain of the human nuclear receptor PPAR gamma”, *J. Biol. Chem.,* **273(47)**, 31108-31112, 1998.

Valasek M.A., Clarke S.L. and Repa J.J., ‘‘Fenofibrate reduces intestinal cholesterol absorption via PPARα-dependent modulation of NPC1L1 expression in mouse,’’ *J. Lipid Res.*, **48**, 2725-2735, 2007.

Vanier M.T., ‘‘Prenatal Diagnosis of Niemann-Pick Diseases Type A, B and C,’’ *Prenat. Diagn.*, **22**, 630-632, 2002.

Vazquez M.C., Balboa E., Alvarez A.R. and Zanlungo S., ‘‘Oxidative Stress: A Pathogenic Mechanism for Niemann-Pick Type C Disease,’’ *Oxid. Med. Cell. Longev.,* 1-11, 2012.

Veen J.R., Kruit J.K., Havinga R., Baller J.F. W., Chimini G., Lestavel S., Staels B., Groot P.H.E., Groen A.K. and Kuipers F., ‘‘Reduced cholesterol absorption upon PPARδ activation coincides with decreased intestinal expression of NPC1L1,’’ *J. Lipid Res.*, **46**, 526-534, 2005.

Voet D., Voet J.G., *Biochemistry*, 3rd edn. John Wiley & Sons Inc., 2004.

Vrins C.L.J., Velde A.E., Oever K., Levels J.H.M., Huet S., Oude Elferink R. P.J., Kuipers F. and Groen A.K., ‘‘Peroxisome proliferator-activated receptor delta activation leads to increased transintestinal cholesterol efflux,’’ *J. Lipid Res.*, **50**, 2009.

Wang A.X., Zheng B.Z., “Macrocyclic Peptides as Hepatitis C Virus Inhibitors”, *WO2008064057 (A1),* 29 May 2008.

Wang L.-J.,Wang J., Li N., Ge L., Li B.-L. andSong B.-L., "Molecular Characterization of the NPC1L1 Variants Identified from Cholesterol Low Absorbers", *J. Biol. Chem.,* **286(9)**, 7397–7408, 2011.

Whitehouse D., Hu S., "Substituted Amino Carboxylic Acids", *WO2006055725 (A2),* 26 May 2006.

Willson T.M., Brown P.J., Sternbach D.D., and Henke B.R., "The PPARs: From Orphan Receptors to Drug Discovery", *J. Med. Chem.,* **43**, 527-550, 2000.

Willson, T.M., Lambert M.H., Kliewer S.A., "Peroxisome proliferator-activated receptor gamma and metabolic disease", *Annu. Rev. Biochem.,* **70**, 341-367, 2001.

Wilson G.G., Abou-Donia M., Frith L., Patel J., Fiedorek F.T., Study Group, PPA 20005. "Monotherapy with GI262570, a tyrosine-based non-thiazolidinedione PPAR-gamma agonist, significantly reduces triglyceride and increases HDL-C concentrations in patients with type 2 diabetes mellitus". Program and Abstracts of the 60th Scientific Sessions of the American Diabetes Association; June 9-13, 2000; San Antonio, Texas. Abstract 158-OR. *Diabetes*, **49**, 39, 2000.

Xu H.E., Lambert M.H., Montana V.G., Parks D.J., Blanchard S.G., Brown P.J., Sternbach D.D., Lehmann J.M., Wisely G.B., Willson T.M., Kliewer S.A., Milburn M.V., "Molecular recognition of fatty acids by peroxisome proliferator-activated receptors", *Mol. Cell,* **3(3)**, 397-403, 1999.

Xu H.E., Lambert M.H., Montana V.G., Plunket K.D., Moore L.B., Collins J.B., Oplinger J.A., Kliewer S.A., Gampe R.T., McKee D.D., Moore J.T., Willson T.M., "Structural determinants of ligand binding selectivity between the peroxisome proliferator-activated receptors", *Proc. Natl. Acad. Sci. USA,* **98(24)**, 13919-13924, 2001.

Xu H.E., Stanley T.B., Montana V.G., Lambert M.H., Shearer B.G., Cobb J.E., McKee D.D., Galardi C.M., Plunket K.D., Nolte R.T., Parks D.J., Moore J.T., Kliewer S.A., Willson T.M., Stimmel J.B., "Structural basis for antagonist-mediated recruitment of nuclear co-repressors by PPAR alpha", *Nature,* **415(6873)**, 813-817, 2002.

Yu L., Bharadwaj S., Brown J. M., Ma Y., Du W., Davis M.A., Michaely P., Liu P., Willingham M.C. and Rudel L.L., ‘‘Cholesterol-regulated Translocation of NPC1L1 to the Cell Surface Facilitates Free Cholesterol Uptake,’’ *J. Biol. Chem.,* **281**, 6616-6624, 2006.